



AVATAR: Reinforcement Learning to See, Hear, and Reason Over Video

Yogesh Kulkarni Pooyan Fazli

Arizona State University

{ykulkar10, pooyan}@asu.edu

<https://people-robots.github.io/AVATAR/>

Abstract

Multimodal reasoning over long-horizon video is challenging due to the need for precise spatiotemporal fusion and alignment across modalities. While recent methods such as Group Relative Policy Optimization (GRPO) have shown promise in this domain, they suffer from three key limitations: (1) data inefficiency from their on-policy design, (2) a vanishing advantage problem, where identical or near-identical rewards within a group eliminate the learning signal by producing zero-valued advantages, and (3) uniform credit assignment that fails to emphasize critical reasoning steps. We introduce AVATAR (Audio-Video Agent for Alignment and Reasoning), a framework that addresses these limitations through two core components: (1) an off-policy training architecture that improves sample efficiency and resolves vanishing advantages by reusing past experiences with greater reward diversity, and (2) Temporal Advantage Shaping (TAS), a novel credit assignment strategy that upweights key reasoning phases during learning. AVATAR achieves strong performance across various benchmarks, outperforming the Qwen2.5-Omni baseline by +5.4 on MMVU, +4.9 on OmniBench, and +4.5 on Video-Holmes, while demonstrating 5× sample efficiency, requiring 80% fewer generated completions to reach target performance.

1. Introduction

Multimodal large language models (MLLMs) must align video, audio, and language modalities to support long-horizon reasoning [36]. This requires balancing dense temporal coverage for narrative understanding with high spatial resolution for visual grounding [3, 26, 65]. Reinforcement learning (RL), particularly Group Relative Policy Optimization (GRPO) [2, 17], has emerged as a promising approach for enhancing such reasoning. However, applying GRPO directly to multimodal domains reveals key limitations.

First, GRPO is an on-policy method, discarding samples

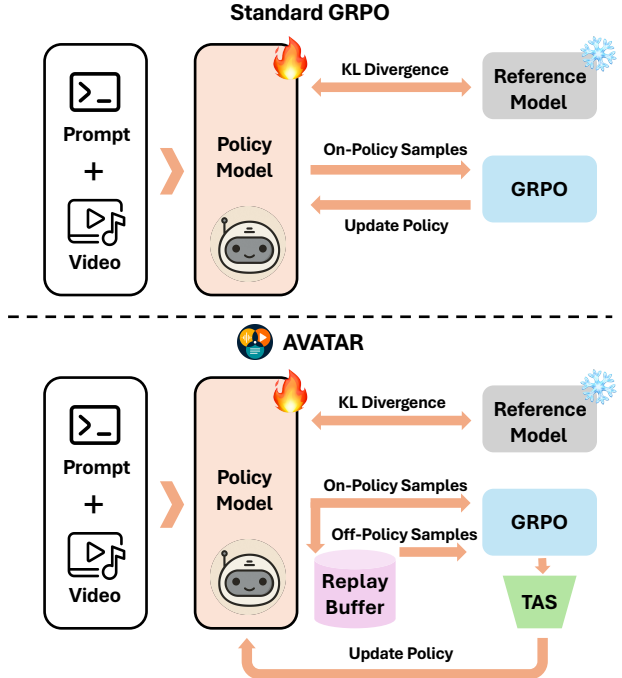


Figure 1. **Standard GRPO (top) vs. AVATAR (bottom).** AVATAR enhances GRPO with two key components: (1) an **off-policy architecture** using a stratified replay buffer to improve data efficiency, and (2) **Temporal Advantage Shaping (TAS)**, a novel credit assignment strategy that focuses learning on critical reasoning steps.

after each update. This makes it data-inefficient, a critical issue in the video domain where learning models rely on expensive, large-scale annotated data [35, 50, 54]. Prior methods like RePO [30] or standard training frameworks like veRL [44] reuse past data but lack selective control over replay quality. **Second**, GRPO suffers from the vanishing advantage problem: when the reward variance within a group collapses, such as in cases where all responses are either uniformly correct or uniformly incorrect, the resulting zero-valued advantage signals prevent effective learning [6, 13, 33, 49]. **Third**, GRPO suffers from uniform credit

assignment [8, 40], assigning the same reward to all tokens in a reasoning chain, regardless of their contribution to the final response [7, 10, 37]. This issue is amplified in multimodal tasks, where the GRPO objective fails to distinguish visually grounded reasoning from plausible text. By treating fluent language and accurate perception as equivalent, the model can produce correct-sounding responses that ignore visual input, resulting in frequent perception errors [11, 53].

To address these challenges, we introduce **AVATAR** (**A**udio-**V**ideo **A**gent for **A**lignment and **R**easoning), a unified framework built on GRPO to enhance multimodal reasoning, with a focus on video tasks. To mitigate GRPO’s data inefficiency, AVATAR adopts an **off-policy training architecture** that reuses past experiences through a stratified replay buffer. Samples are grouped based on how often the policy has succeeded on them in the past. This creates a curriculum that helps the model focus on samples it previously failed on, which is especially important for learning from sparse and challenging audio-video data. Moreover, to enhance training stability and the quality of the reward signal, we build upon prior clue-grounded reward formulations [20, 25, 36], which evaluate whether the model leverages relevant audio or visual cues from the query.

We also address the uniform credit assignment problem with a new method called **Temporal Advantage Shaping (TAS)**. Unlike prior work that treats all tokens equally [40] or depends on statistical variance [7], TAS guides learning based on a token’s position in the reasoning chain, placing greater weight on the beginning (planning) and end (synthesis) stages. This is especially useful for audio-video tasks, where accurate early grounding (e.g., locating the speaker) and final synthesis (e.g., combining speech and visual cues to identify the speaker) are critical. In the experiments, we apply AVATAR within a three-stage RL training pipeline to evaluate its effectiveness: starting with general visual reasoning, followed by audio-visual alignment, and concluding with fine-grained audio-based object localization. In summary, our primary contributions are:

1. We present **AVATAR**, an off-policy RL framework designed to improve data efficiency in audio-video reasoning by leveraging past experiences through a difficulty-aware replay buffer that prioritizes challenging samples.
2. We introduce new approaches for reinforcement learning reward signaling and credit assignment by allocating partial credit to intermediate reasoning steps, stabilizing learning through a moving average of past rewards, and emphasizing the critical components of reasoning.
3. Experiments show that **AVATAR** achieves significant gains over the Qwen2.5 Omni baseline, with improvements of +5.4 on MMVU, +4.9 on OmniBench, and +4.5 on Video-Holmes, while requiring 80% fewer generated completions to reach target performance.

2. Related Work

Multimodal Understanding. Recent MLLMs have made remarkable progress towards audio-video understanding [1, 14, 22, 45, 46, 68]. Key efforts focus on architectural enhancements such as dedicated audio branches and video connectors [5], using clue aggregators to ground responses in question-specific details [61], or with token interleaving to enhance temporal understanding [46]. However, these methods excel at direct video question answering but cannot rationalize their thoughts through reasoning traces. This limitation is problematic for complex audio-visual tasks requiring multi-step reasoning and fine-grained cross-modal alignment, such as localizing sound sources. In contrast, AVATAR enhances structured reasoning capabilities in audio-visual models using a sample-efficient RL approach.

Multimodal Understanding with RL. Early multimodal efforts use preference optimization like DPO [23, 24, 39, 42], but RL methods such as GRPO [2, 17] have shown greater promise for reasoning. Recent variants adapt GRPO to specific tasks: Video-R1 uses temporal contrastive rewards [12], HumanOmniV2 employs LLM-judged rewards for global audio-visual context [62], Omni-R1 targets audio-visual segmentation [65], and GRIT generates spatial reasoning chains [11]. However, these approaches suffer from uniform credit assignment and sample inefficiency. AVATAR addresses these limitations through its off-policy architecture and TAS credit assignment. For audio-visual tasks, its temporal weighting emphasizes early grounding (localizing sounds) and late synthesis (combining auditory and visual evidence), while the stratified replay buffer handles sparse cross-modal data effectively.

3. Preliminaries

3.1. Group Relative Policy Optimization

GRPO is an RL framework that can be used to fine-tune MLLMs by comparing multiple candidate responses generated by a behavior policy $\pi_{\theta_{\text{old}}}$ for a given prompt q [17]. Each candidate output o_i typically includes both intermediate reasoning steps and a final answer. For each group of K candidate responses $\{o_i\}_{i=1}^K$, scalar rewards $R(o_i)$ from predefined reward functions are assigned to each response. These rewards are then normalized within the group to obtain relative advantages A_i .

$$A_i = \frac{R(o_i) - \mu_R}{\sigma_R + \epsilon_{\text{adv}}}, \quad (1)$$

where μ_R and σ_R are the mean and standard deviation of the group rewards $\{R(o_i)\}_{i=1}^K$ and ϵ_{adv} is a small constant for numerical stability. These group-relative advantages guide the update of the target policy π_{θ} , encouraging it to assign higher probability to relatively better responses. GRPO

maximizes the following clipped surrogate objective with KL regularization [30]:

$$\mathcal{J}_{\text{GRPO}}(\theta) = \mathbb{E}_{\substack{q \sim \mathcal{D} \\ \{o_i\}_{i=1}^K \sim \pi_{\theta_{\text{old}}}}} \left[\frac{1}{K} \sum_{i=1}^K \min(r_i A_i, \bar{r}_i A_i) - \beta D_{\text{KL}}(\pi_{\theta}(\cdot|q) \parallel \pi_{\text{ref}}(\cdot|q)) \right], \quad (2)$$

where $\bar{r}_i = \text{clip}(r_i, 1 - \epsilon, 1 + \epsilon)$, q is a prompt sampled from the dataset \mathcal{D} , r_i is the importance sampling ratio $\frac{\pi_{\theta}(o_i|q)}{\pi_{\theta_{\text{old}}}(o_i|q)}$, ϵ controls the clipping range, and β weights the KL divergence term to ensure stability by regularizing the updated policy π_{θ} against a reference policy π_{ref} . Here, π_{ref} refers to the pretrained model before RL fine-tuning, used to prevent large deviations from the original policy.

3.2. GRPO Limitations

Data Inefficiency Problem. GRPO is an on-policy method that discards experiences after a single update, a highly inefficient design for audio-visual reasoning, which relies on scarce, costly annotated data. When the pre-trained policy struggles with a complex prompt, this on-policy nature forces it to “move on,” discarding the informative failure experience instead of learning from it. Off-policy updates offer a more efficient alternative by creating a memory of these past experiences, enabling repeated learning on the most challenging samples.

Vanishing Advantage Problem. A fundamental limitation of GRPO arises from its advantage estimation mechanism. When the rewards $R(o_i)$ for all outputs in a group are identical or nearly identical (e.g., all zero for a particularly difficult prompt or all one for an easy prompt), the group mean baseline μ_R equals each reward. As a result, the advantages become zero for all samples i : $A_i = R(o_i) - \mu_R = 0$. This eliminates the learning signal and prevents the policy from updating. Consequently, GRPO fails to learn from such training samples, a phenomenon referred to as the *vanishing advantage problem* [30, 49].

Credit Assignment Problem. Another key limitation of GRPO is its overly simplistic credit assignment. In Equation 2, a single scalar advantage A_i is computed for the entire output o_i and applied uniformly to all tokens during policy updates. This ignores the varying importance of different reasoning steps or temporal phases. Tokens critical to initial planning receive the same learning signal as those from less important phases, failing to address the temporal credit assignment challenge that RL is designed to solve.

Algorithm 1 AVATAR

- 1: **Input:** Initial policy $\pi_{\theta_{\text{init}}}$, Rewards R , Hyperparams $\alpha, \lambda_{\text{TAS}}, \beta, \epsilon, K_{\text{on}}, K_{\text{off}}$.
 - 2: **Initialize:** $\pi_{\theta} \leftarrow \pi_{\theta_{\text{init}}}$, $\pi_{\text{ref}} \leftarrow \pi_{\theta_{\text{init}}}$, empty Buffer \mathcal{B} , VCRS $\bar{R}(q) \leftarrow \{\}$.
 - 3: **for** each training step **do**
 - 4: Sample prompts Q_{batch} ; $\pi_{\theta_{\text{old}}} \leftarrow \pi_{\theta}$
 - 5: Generate K_{on} on-policy $E_{\text{on}} = \{(q, o, R(o))\}$ using $\pi_{\theta_{\text{old}}}$; Compute A_{on} (Eq. 1).
 - 6: Retrieve VCRS $\bar{R}(q)$; Sample K_{off} off-policy $E_{\text{off}} = \{(q, o, R(o), \pi_{\theta_{\text{off}}})\}$ from \mathcal{B} ; Compute A_{off} using $\bar{R}(q)$ (Eq. 11).
 - 7: Compute shaped advantages $A_{i,t}^{\text{TAS}} \leftarrow (A_{\text{on}} \cup A_{\text{off}}) \cdot w_{i,t}$ using TAS weights $w_{i,t}$ (Eq. 6).
 - 8: Compute $\mathcal{J}_{\text{total}}(\theta)$ using $A_{\text{on}}^{\text{TAS}}, A_{\text{off}}^{\text{TAS}}$ and importance ratios $r_i^{\text{on}}, r_i^{\text{off}}$ (Eq. 3).
 - 9: Update policy: $\theta \leftarrow \theta - \eta \nabla_{\theta} \mathcal{J}_{\text{total}}(\theta)$.
 - 10: Update \mathcal{B} with E_{on} (with stratification/hinting); Update $\bar{R}(q)$ using E_{on} .
 - 11: **end for**
-

4. AVATAR

We introduce AVATAR, an off-policy RL framework for multimodal alignment and reasoning, designed to address key limitations of GRPO. To tackle the vanishing advantage problem and resulting data inefficiency, AVATAR employs an *off-policy* training architecture using a *stratified replay buffer*. To overcome uniform credit assignment, it introduces *Temporal Advantage Shaping (TAS)*, which modulates advantages across the reasoning sequence by upweighting tokens at the beginning and end of the sequence, ensuring that critical planning and final decision steps receive stronger learning signals.

4.1. Off-Policy Architecture

To address both the data inefficiency of on-policy learning and the vanishing advantage problem, AVATAR employs an off-policy architecture.

Replay Buffer. We employ a stratified replay buffer \mathcal{B} to improve sample efficiency via a progressive curriculum. The buffer of size $10k$ is divided into three fixed-capacity tiers based on difficulty: Easy (25%), Medium (35%), and Hard (40%). At each training step, new experiences $(q, o, \pi_{\theta_{\text{off}}})$, required for off-policy importance sampling, are stored. Tier assignment is determined not by individual rewards, but by the prompt’s moving average reward $\bar{R}(q)$, which serves as a dynamic difficulty metric. The tier thresholds are dynamic quantiles based on the $\bar{R}(q)$ score distribution, assigning the bottom 40% of experiences to ‘Hard’, the next 35% to ‘Medium’, and the top 25% to ‘Easy’. As the agent’s

performance on a prompt q improves, its $\bar{R}(q)$ rises, and new experiences for that prompt are promoted to easier tiers. This curriculum design ensures difficult samples (low $\bar{R}(q)$) are retained in the high-capacity ‘Hard’ tier, forcing the model to learn from its failure modes through repeated exposure.

Hinting Mechanism. AVATAR leverages the KL divergence $D_{KL}(\pi_\theta, \cdot | \pi_\beta)$ between the target policy π_θ and behavior policy π_β to monitor policy stability. When a prompt remains hard (low $\bar{R}(q)$) and the policy stops exploring (low KL), a pre-computed *hint* is triggered. Hints (e.g., “first locate the object making the sound, then count”) are generated by providing the full problem context (video, audio caption, query, and ground truth) to Qwen2.5-VL [1] and are used as additional guidance to help the agent escape local optima. This ensures training remains in a challenging but solvable regime while promoting targeted exploration [20]. Prompt provided in Supplementary, Figure 13.

Hybrid Training with Selective Replay. At each training step, a batch is formed from both newly generated on-policy samples and off-policy samples from the replay buffer. We empirically determined an optimal 4:4 ratio for this through hyperparameter tuning, detailed in Supplementary Figure 7. To correct for policy drift in off-policy data, we apply importance sampling. The full objective for AVATAR combines the standard on-policy GRPO loss (Equation 2) with a corrected off-policy term:

$$\mathcal{J}_{\text{AVATAR}}(\theta) = \mathcal{J}_{\text{on-policy}}(\theta) + \alpha \cdot \mathcal{J}_{\text{off-policy}}(\theta), \quad (3)$$

where α controls the off-policy contribution. The off-policy objective $\mathcal{J}_{\text{off-policy}}$ follows the same form as Equation 2, but uses an importance sampling ratio based on the behavior policy $\pi_{\theta_{\text{off}}}$ that generated the replayed samples:

$$r_i^{\text{off}}(\theta) = \frac{\pi_\theta(o_i|q)}{\pi_{\theta_{\text{off}}}(o_i|q)}. \quad (4)$$

Prior works [30, 49] use generic replay strategies or standard advantage calculations for off-policy data whereas AVATAR introduces a difficulty-aware stratified buffer for curriculum learning and employs the VCRS baseline (Eq. 11) to stabilize advantage estimation specifically for these replayed samples. The full procedure is detailed in Algorithm 1.

4.2. Temporal Advantage Shaping (TAS)

Standard GRPO employs uniform credit assignment, applying the same sequence-level advantage A_i to every token (Eq. 2), which struggles to differentiate crucial reasoning steps in complex tasks. Recent work [38, 57] demonstrates that *not all tokens contribute equally*: GRPO- λ [38] shows that rapid value propagation to earlier tokens significantly improves learning, while process-based credit assignment [57] reveals

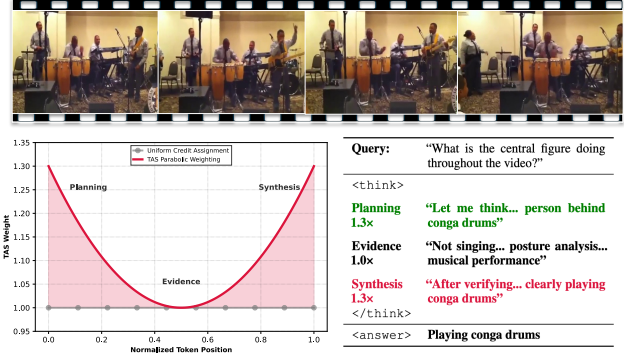


Figure 2. To address GRPO’s uniform credit assignment (gray line), TAS applies a parabolic weighting function to amplify advantages during crucial **planning** and **synthesis** stages.

that tokens at critical decision points warrant stronger learning signals. For audio-visual reasoning requiring tight cross-modal coupling, this token-level differentiation becomes even more critical, like humans who devote disproportionate cognitive effort to planning how to align modalities and synthesizing multimodal evidence, rather than processing intermediate unimodal features. Motivated by these findings, we introduce Temporal Advantage Shaping (TAS), a simple, critic-free modification to GRPO. Reasoning often follows a planning-evidence-synthesis structure, reinforced during SFT. TAS leverages this by hypothesizing that planning and synthesis tokens are most critical. It modulates the learning signal based on relative token position, upweighting the sequence’s beginning and end, aligning with findings favoring non-uniform weighting [38]. As shown in Figure 2, TAS uses a U-shaped parabolic function w_t to yield a token-specific shaped advantage, $A_{i,t}^{\text{TAS}} = w_{i,t} \cdot A_i$. This focuses learning on key reasoning phases, reinforcing critical steps without overemphasizing intermediate tokens.

Parabolic Weighting Function. For a reasoning sequence of length L , we normalize each token’s position $t \in \{0, 1, \dots, L-1\}$ to the range $[0, 1]$ by defining

$$\tilde{t} = \frac{t}{L-1}. \quad (5)$$

We then compute a token-specific weight using a parabolic function,

$$w_t = 1.0 + \lambda_{\text{TAS}} \cdot (2\tilde{t} - 1)^2, \quad (6)$$

where λ_{TAS} controls the amplitude of the weight variation. This function assigns the minimum weight of 1.0 to tokens at the midpoint of the sequence ($\tilde{t} = 0.5$) and the maximum weight of $1.0 + \lambda_{\text{TAS}}$ to tokens at the start and end ($\tilde{t} = 0$ or 1). These weights define a token-specific shaped advantage: $A_{i,t}^{\text{TAS}} = w_{i,t} \cdot A_i$, where $i \in \{1, \dots, K\}$ indexes each of the K candidate responses in the group. AVATAR’s loss is

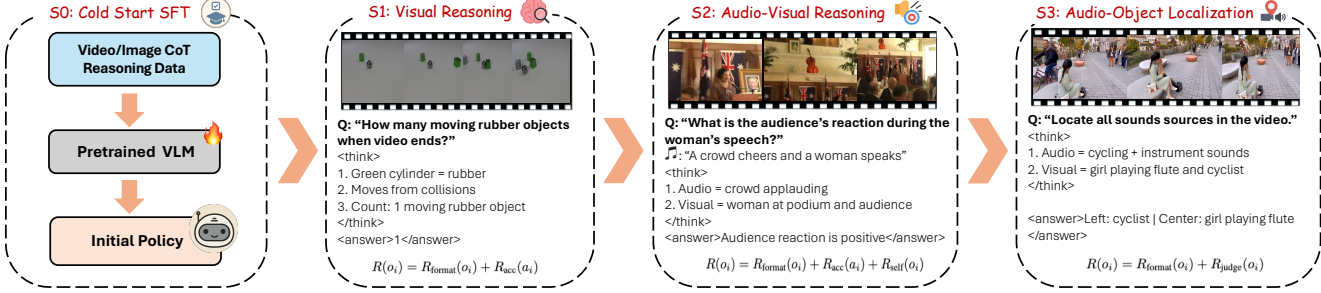


Figure 3. **Three-stage RL training pipeline to evaluate AVATAR.** The framework advances from **Cold start SFT** (Stage 0) to **Visual Reasoning** (Stage 1) to **Audio-Visual Reasoning** (Stage 2) to **Audio-Object Localization** (Stage 3).

formed by replacing the standard GRPO advantage A_i in Equation 2 with this shaped advantage. Reasoning sequence lengths, L_i , vary across completions, which can affect positional weighting. However, the TAS mechanism remains robust because the normalization in Equation 5 ensures that each token’s weight depends on its relative position \tilde{t} within the sequence rather than its absolute position.

4.3. Reward Functions

AVATAR is guided by a set of reward functions as detailed below:

(1) Format Reward (R_{format}). A binary reward that verifies adherence to the predefined reasoning format (i.e., $<\text{think}>\dots</\text{think}><\text{answer}>\dots</\text{answer}>$).

$$R_{\text{format}}(o_i) = \begin{cases} 1, & \text{if format is correct} \\ -1, & \text{otherwise} \end{cases} \quad (7)$$

(2) Final Answer Accuracy (R_{acc}). A black-box evaluation of the final answer a_i extracted from the $<\text{answer}>$ tag, compared to the ground truth a_{GT} . For non-zero numerical tasks, we use the relative Mean Absolute Error (rMAE) for a dense reward signal [36].

$$R_{\text{acc}}(a_i) = 1.0 - \min \left(1.0, \frac{|a_i - a_{\text{GT}}|}{a_{\text{GT}}} \right) \quad (8)$$

(3) Self-Rewarding (R_{self}). We use self-rewarding to help the model learn from its own consensus. Given a group of K generated answers $\{o_1, o_2, \dots, o_K\}$ for a prompt, we choose the most common answer as a “pseudo-correct” o_{maj}^* one using majority vote. Ties are broken by choosing the response with the highest model confidence (average token likelihood).

$$o_{\text{maj}}^* = \operatorname{argmax}_{o \in \{o_1, \dots, o_K\}} \sum_{i=1}^K \mathbb{I}(o_i = o), \quad (9)$$

where \mathbb{I} is the indicator function. The self-reward for each answer o_i is then a binary score based on its agreement with

this consensus:

$$R_{\text{self}}(o_i) = \begin{cases} 1, & \text{if } o_i = o_{\text{maj}}^* \\ 0, & \text{otherwise} \end{cases} \quad (10)$$

(4) Stepwise Reasoning Judge (R_{judge}). A white-box reward from a frozen VLM judge (InternVL3 [68]), which provides a detailed score for reasoning quality within the $<\text{think}>$ block. It evaluates logical consistency and correct use of grounding clues from the prompt. The score $s_{\text{judge}} \in [0, 1]$ reflects the reasoning process quality independently of the final answer. The judge prompt is provided in Supplementary, Figure 14.

4.4. Video-Context Reference Score (VCRS)

Standard off-policy updates can be noisy, as the group mean (μ_R) is an unstable baseline for stale buffer samples. We stabilize learning by introducing VCRS, denoted as $\bar{R}(q)$, which is a stable moving average of rewards for a prompt q computed over its last 20 new (on-policy) instances.

This stable score $\bar{R}(q)$ replaces the noisy μ_R in the off-policy advantage calculation:

$$A_{i,\text{off}} = \frac{R(o_i) - \bar{R}(q)}{\sigma_{R,\text{off}}}, \quad (11)$$

where $\sigma_{R,\text{off}}$ is the standard deviation of the off-policy batch. This provides a reliable advantage signal, prevents stagnation, and makes the GRPO process more robust. This final advantage $A_{i,\text{off}}$ is then modulated by TAS.

5. Experiments

Implementation Details. We evaluate AVATAR on Qwen2.5-Omni-7B [59] and Ola-7B [34], two open-source

Table 1. Dataset and Reward Configuration for AVATAR Training.

Stage	Focus	Datasets	Reward Components
S0: SFT	Cold Start	Video-R1-CoT [12], TPO [29]	N/A (Supervised)
S1: RL	Visual Reasoning	Video-R1 [12]	$0.5 \times R_{\text{format}} + 0.5 \times R_{\text{acc}}$
S2: RL	Audio-Visual Reasoning	AVQA [60], AVE [47]	$0.2 \times R_{\text{format}} + 0.4 \times R_{\text{acc}} + 0.4 \times R_{\text{self}}$
S3: RL	Audio-Object Localization	AVSBench [66]	$0.2 \times R_{\text{format}} + 0.4 \times R_{\text{acc}} + 0.4 \times R_{\text{judge}}$

Table 2. **Comprehensive evaluation of AVATAR vs. state-of-the-art audio-video understanding models.** Best scores are in **bold**, and second-best scores are underlined. Performance improvements from applying AVATAR to a baseline model are shown in **green** with 95% confidence interval (CI) margins (\pm) computed via bootstrap resampling (10,000 iterations, percentile method). Improvements are statistically significant at $\alpha = 0.05$ when CIs exclude zero. All results were reproduced by us; * denotes potential data contamination.

Model	OmniBench	DailyOmni	AV-Counting	AV-Odyssey	WorldSense	IntentBench
<i>State-of-the-Art Models</i>						
EchoInk [58]	46.5	46.2	22.7	31.1	<u>45.7</u>	63.6
Omni-R1 [65]	46.9	46.8	22.0	<u>31.2</u>	44.1	63.5
HumanOmni [62]	44.9	47.6	19.6	30.3	45.4	*
AV-Reasoner [36]	<u>48.3</u>	<u>53.8</u>	<u>23.0</u>	25.6	44.6	59.5
<i>Model-Agnostic Reinforcement Learning with AVATAR</i>						
Ola-7B [34] (Baseline)	45.3	52.3	17.4	25.6	44.2	59.1
+ AVATAR	47.2 ($+1.9 \pm 0.5$)	55.7 ($+3.4 \pm 0.7$)	19.5 ($+2.1 \pm 0.6$)	28.8 ($+3.2 \pm 0.6$)	45.0 ($+0.8 \pm 0.4$)	61.9 ($+2.8 \pm 0.6$)
Qwen2.5-Omni [59] (Baseline)	44.2	44.0	22.3	29.8	44.2	<u>63.7</u>
+ AVATAR	49.1 ($+4.9 \pm 0.7$)	47.0 ($+3.0 \pm 0.6$)	23.1 ($+0.8 \pm 0.4$)	32.1 ($+2.3 \pm 0.6$)	46.0 ($+1.8 \pm 0.5$)	63.9 ($+0.2 \pm 0.1$)

Table 3. **Comprehensive evaluation of AVATAR on video understanding and reasoning benchmarks.** Best scores are in **bold**, and second-best scores are underlined. Performance improvements from applying AVATAR to a baseline model are shown in **green** with 95% confidence interval (CI) margins (\pm) computed via bootstrap resampling (10,000 iterations, percentile method). Improvements are statistically significant at $\alpha = 0.05$ when CIs exclude zero. \dagger Improvement not statistically significant ($p > 0.05$; 95% CI includes zero).

Model	General Video Understanding			Video Reasoning		
	MVBench	Video-MME	LVBench	Video-Holmes	MMVU	TOMATO
<i>State-of-the-Art Models</i>						
EchoInk [58]	<u>66.2</u>	60.8	<u>37.6</u>	42.5	65.7	<u>29.9</u>
Omni-R1 [65]	66.0	60.7	<u>37.6</u>	<u>44.2</u>	63.6	29.2
HumanOmni [62]	61.4	63.1	36.2	39.6	61.8	27.1
AV-Reasoner [36]	47.9	56.8	33.7	39.6	57.9	24.9
Qwen2.5-VL [1]	59.4	60.1	31.2	38.0	61.9	29.3
Video-R1 [12]	63.9	59.3	27.8	41.0	63.1	19.8
VideoRFT [50]	62.1	59.8	34.2	40.5	58.0	20.6
TW-GRPO [7]	63.3	60.1	33.8	38.4	61.4	23.5
<i>Model-Agnostic Reinforcement Learning with AVATAR</i>						
Ola-7B [34] (Baseline)	40.1	59.1	35.5	40.1	56.6	25.3
+ AVATAR	45.4 ($+5.3 \pm 0.8$)	61.4 ($+2.3 \pm 0.6$)	36.6 ($+1.1 \pm 0.5$)	42.4 ($+2.3 \pm 0.6$)	57.3 ($+0.7 \pm 0.4$)	26.6 ($+1.3 \pm 0.5$)
Qwen2.5-Omni [59] (Baseline)	66.1	58.3	37.2	40.6	60.2	29.0
+ AVATAR	66.4 ($+0.3 \pm 0.3$) \dagger	62.8 ($+4.5 \pm 0.7$)	38.4 ($+1.2 \pm 0.5$)	45.1 ($+4.5 \pm 0.7$)	<u>65.6</u> ($+5.4 \pm 0.8$)	30.8 ($+1.8 \pm 0.5$)

MLLMs that provide native audio and video support and are the current SOTA in this space. We implement AVATAR using the MS-Swift [63] framework for GRPO training. Our training follows the curriculum detailed in Table 1 and Figure 3, beginning with a cold-start SFT phase (S0) followed by three RL stages (S1-S3) of increasing complexity, each targeting different reasoning skills using specific datasets and reward configurations. Stage 2 uses audio cues annotated via Kimi-Audio [9], and Stage 3 employs stepwise rewards from an InternVL3 [68] judge. We uniformly sample 32 video frames during both training and evaluation. TAS is applied throughout all RL stages.

We attach LoRA [19] adapters to the Vision Encoder, Audio Encoder, MLP, and the LLM with parameters $r = 16$ and $\alpha_{\text{LoRA}} = 32$. The key hyperparameters for AVATAR are $\lambda_{\text{TAS}} = 0.3$, $\alpha = 0.6$, $\beta = 0.1$.

State-of-the-art Models. We compare AVATAR with a broad range of models across audio-visual and video-only modalities. For audio-visual models, we evaluate against Qwen2.5-Omni-7B [59], EchoInk [58], Omni-R1 [65], HumanOmni [62], Ola-7B [34], and AV-Reasoner [36]. To assess the impact of audio integration, we also compare with SOTA video-only models: Qwen2.5VL [1], Video-R1 [12], Video-RFT [50], and TW-GRPO [7].

Table 4. **Component-wise ablation** demonstrating how each component addresses specific GRPO limitations. The **stratified replay buffer** resolves data inefficiency and vanishing advantages, **TAS** improves credit assignment, and **hinting** helps escape local optima.

Model Configuration	Audio-Visual Benchmarks			Video Reasoning Benchmarks		
	OmniBench	DailyOmni	AV-Odyssey	Video-Holmes	MMVU	TOMATO
Qwen2.5 Omni	44.2	44.0	29.8	40.6	60.2	29.0
GRPO	45.4 (+1.2)	44.8 (+0.8)	31.3 (+1.5)	43.2 (+2.6)	64.0 (+3.8)	29.2 (+0.2)
+ TAS Only (w/ On-Policy GRPO)	45.1 (+0.9)	45.4 (+1.4)	31.4 (+1.6)	43.4 (+2.8)	64.3 (+4.1)	29.5 (+0.5)
+ Replay Buffer (w/ Uniform Credit)	47.8 (+3.6)	45.9 (+1.9)	31.6 (+1.8)	43.7 (+3.1)	64.8 (+4.6)	29.3 (+0.3)
AVATAR (w/o Hinting)	48.2 (+4.0)	46.1 (+2.1)	31.8 (+2.0)	44.3 (+3.7)	65.0 (+4.8)	30.2 (+1.2)
AVATAR (w/ Hinting)	49.1 (+4.9)	47.0 (+3.0)	32.1 (+2.3)	45.1 (+4.5)	65.6 (+5.4)	30.8 (+1.8)

Benchmarks. For audio-visual tasks, we use OmniBench [31] (image-audio-text reasoning), DailyOmni [67] (ambient sound scenarios), AV-Counting [36] (cross-modal counting), AV-Odyssey [16] (audio-visual alignment), WorldSense [18] (omnimodal understanding in-the-wild), and IntentBench [62] (reasoning about human intent and actions). For video understanding and reasoning, we evaluate on MVBench [28] (temporal perception-to-cognition QA), Video-MME [15] (full-spectrum video comprehension), LVbench [52] (long-video reasoning), Video-Holmes [4] (causal inference in suspense clips), MMVU [64] (domain-expert knowledge analysis), and TOMATO [43] (temporal reasoning).

5.1. Results

Audio-Visual Reasoning. As shown in Table 2, AVATAR substantially improves audio-visual reasoning over baselines like Qwen2.5-Omni (+4.9 on OmniBench, +3.0 on DailyOmni) and Ola-7B (+3.4 on DailyOmni, +3.2 on AV-Odyssey). Our stratified replay buffer addresses GRPO’s vanishing advantage issue, preventing stalling and overfitting and outperforming methods like AV-Reasoner and Omni-R1. TAS further enhances performance on benchmarks that require precise temporal alignment, such as AV-Odyssey. By upweighting tokens at the sequence start and end, TAS is designed to reinforce the critical reasoning steps such as early audio grounding and final cross-modal integration needed for such tasks.

General Video Understanding and Reasoning. AVATAR demonstrates strong performance on general video understanding benchmarks like MVBench (+5.3 w/ Ola) and VideoMME (+4.5 w/ Qwen), and excels in complex reasoning (Table 3). It achieves significant gains on causal inference tasks such as Video-Holmes (+4.5) and MMVU (+5.4). These improvements stem from the stratified replay buffer ensuring exposure to hard examples and TAS guiding reasoning by emphasizing planning and synthesis phases. Unlike unstable statistical weighting methods (e.g., TW-GRPO [7] on TOMATO), TAS leverages temporal structure

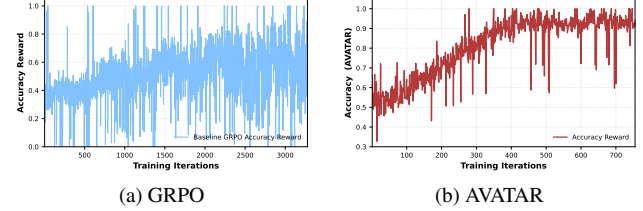


Figure 4. Comparison of training dynamics between GRPO and AVATAR. (a) shows **oscillatory and unstable accuracy reward progression**, whereas AVATAR (b) demonstrates a **smoother, more consistent learning trajectory**.

for a stable learning signal, yielding consistent top performance.

5.2. Ablation Studies

RQ1: How efficient is AVATAR? AVATAR reaches 0.80 accuracy in 400 iterations (1,600 unique completions), while baseline GRPO fails to reach this performance even after 1,000 iterations (8,000 unique completions), achieving 5× greater sample efficiency (Figure 4). GRPO exhibits frequent reward collapses to zero, reflecting the vanishing advantage problem, while AVATAR never drops below 0.3. By maintaining reward diversity within each training group, AVATAR avoids uniform-failure scenarios that stall learning and reduces sample requirements by 80%.

RQ2: What is the effect of each component in AVATAR? Our component-wise ablation study (Table 4) isolates how each part of AVATAR addresses specific GRPO limitations. Introducing the replay buffer significantly boosts performance over baseline GRPO (e.g., +3.6 on OmniBench), confirming its effectiveness in tackling data inefficiency and the vanishing advantage problem by enabling off-policy learning, even with uniform credit assignment. Conversely, adding TAS to standard on-policy GRPO also yields gains (e.g., +4.1 on MMVU) over baseline GRPO, demonstrating its ability to improve performance solely by resolving uniform credit assignment. Combining both the replay buffer and

Table 5. **Ablation studies on training curriculum and advantage shaping strategies.** TAS significantly outperforms uniform weights and inverse parabolic weights, validating our hypothesis that **early** and **late** reasoning phases are most critical.

Ablation Configuration		OmniBench	Audio-Visual			Video Reasoning	
Group	Setting		DailyOmni	AV-Odyssey	Video-Holmes	MMVU	TOMATO
Qwen2.5 Omni		44.2	44.0	29.8	40.6	60.2	29.0
Training Curriculum	SFT Only	45.8 (+1.6)	45.2 (+1.2)	30.1 (+0.3)	41.8 (+1.2)	62.1 (+1.9)	28.9 (-0.1)
	SFT + Stage 1 RL	47.2 (+3.0)	45.8 (+1.8)	30.6 (+0.8)	43.5 (+2.9)	64.2 (+4.0)	29.4 (+0.4)
	SFT + Stages 1+2 RL	48.6 (+4.4)	46.7 (+2.7)	31.8 (+2.0)	44.2 (+3.6)	65.1 (+4.9)	30.1 (+1.1)
	SFT + Stages 1+2+3 RL (Ours)	49.1 (+4.9)	47.0 (+3.0)	32.1 (+2.3)	45.1 (+4.5)	65.6 (+5.4)	30.8 (+1.8)
Advantage Shaping	Linear Decay Weights	48.3 (+4.1)	46.2 (+2.2)	31.6 (+1.8)	44.3 (+3.7)	64.8 (+4.6)	30.2 (+1.2)
	Linear Incline Weights	48.5 (+4.3)	46.4 (+2.4)	31.7 (+1.9)	44.6 (+4.0)	65.0 (+4.8)	30.4 (+1.4)
	Uniform Weights (Baseline GRPO)	47.8 (+3.6)	45.9 (+1.9)	31.6 (+1.8)	43.7 (+3.1)	64.8 (+4.6)	29.3 (+0.3)
	Inverse Parabolic Weights	46.5 (+2.3)	45.1 (+1.1)	30.8 (+1.0)	42.8 (+2.2)	63.5 (+3.3)	29.1 (+0.1)
	TAS (Ours)	49.1 (+4.9)	47.0 (+3.0)	32.1 (+2.3)	45.1 (+4.5)	65.6 (+5.4)	30.8 (+1.8)

Table 6. **Ablation comparing the impact of SFT and AVATAR integration.** Models trained with SFT achieve **stronger cross-modal grounding and reward alignment**, while removing SFT leads to significant degradation in both GRPO and AVATAR.

Setting	Audio-Visual Benchmarks		
	OmniBench	DailyOmni	AV-Odyssey
Qwen2.5 Omni	44.2	44.0	29.8
GRPO (w/o SFT)	41.2 (-3.0)	40.8 (-3.2)	27.1 (-2.7)
GRPO (w/ SFT)	46.0 (+1.8)	45.5 (+1.5)	30.2 (+0.4)
AVATAR (w/o SFT)	43.8 (-0.4)	43.5 (-0.5)	28.9 (-0.9)
AVATAR (w/ SFT)	49.1 (+4.9)	47.0 (+3.0)	32.1 (+2.3)

TAS results in further improvements, as the buffer provides better data while TAS ensures effective learning from it. Finally, adding the hinting mechanism provides an additional performance lift, validating its role in helping the model escape challenging local optima.

RQ3: What is the effect of the training curriculum and advantage shaping? Table 5 validates the effectiveness of both the staged training curriculum and the TAS strategy. The curriculum shows consistent stage-wise improvements: Stage 1 RL strengthens visual reasoning over SFT, Stage 2 adds cross-modal alignment, and Stage 3 refines fine-grained localization, yielding progressive gains in reasoning ability. The advantage shaping ablation compares several weighting schemes: uniform (GRPO baseline), linear decay (planning-focused), linear incline (synthesis-focused), inverse parabolic (middle-focused), and our parabolic TAS (planning and synthesis-focused). Results confirm that extreme emphasis on either phase or the middle yields inferior results, while TAS achieves the best overall performance by jointly amplifying early planning and late synthesis steps.

RQ4: Effect of SFT on Learning Stability. Table 6 shows that incorporating SFT before GRPO provides essential struc-

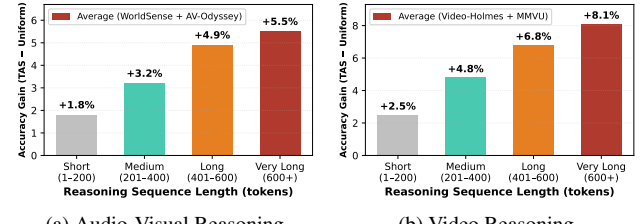


Figure 5. **Effect of reasoning sequence length on TAS performance.** In both (a) audio-visual and (b) video reasoning benchmarks, TAS yields greater gains with longer reasoning sequences.

tural grounding that improves convergence and generalization. Without SFT, models lack cross-modal alignment, resulting in unstable rewards and degraded performance across all benchmarks. Initializing GRPO from an SFT-trained policy yields more stable learning and moderate gains, while AVATAR achieves the highest improvements. Hence, SFT establishes a reliable foundation for stable advantage estimation and TAS-based reward shaping, enabling GRPO to refine rather than relearn multimodal reasoning.

RQ5: Impact of TAS across Reasoning Lengths. As shown in Figure 5, TAS consistently improves performance across reasoning lengths, with gains amplifying as sequences grow longer. The advantage becomes more pronounced for extended sequences (400+ tokens), particularly on challenging benchmarks like MMVU and Video-Holmes. This highlights TAS’s ability to preserve credit assignment and stabilize optimization in long-horizon reasoning, where uniform credit tends to dilute reward signals.

6. Conclusion

We introduce AVATAR, an RL framework that addresses key limitations of GRPO in multimodal audio-video reasoning.

Our primary finding is that jointly addressing data inefficiency and uniform credit assignment is essential for robust performance. We show that an off-policy curriculum with a stratified replay buffer outperforms standard on-policy methods, while TAS significantly enhances reasoning quality by emphasizing critical planning and synthesis phases.

Acknowledgments

This research was supported by the National Eye Institute (NEI) of the National Institutes of Health (NIH) under award number R01EY034562. The content is solely the responsibility of the authors and does not necessarily represent the official views of the NIH.

References

- [1] Shuai Bai, Keqin Chen, Xuejing Liu, Jialin Wang, Wenbin Ge, Sibo Song, Kai Dang, Peng Wang, Shijie Wang, Jun Tang, et al. Qwen2. 5-vl technical report. *arXiv preprint arXiv:2502.13923*, 2025. [2](#), [4](#), [6](#)
- [2] Hardy Chen, Haoqin Tu, Fali Wang, Hui Liu, Xianfeng Tang, Xinya Du, Yuyin Zhou, and Cihang Xie. Sft or rl? an early investigation into training rl-like reasoning large vision-language models. *Transactions on Machine Learning Research*, 2025. [1](#), [2](#)
- [3] Yukang Chen, Wei Huang, Baifeng Shi, Qinghao Hu, Hanrong Ye, Ligeng Zhu, Zhijian Liu, Pavlo Molchanov, Jan Kautz, Xiaojuan Qi, Sifei Liu, Hongxu Yin, Yao Lu, and Song Han. Scaling rl to long videos. In *Advances in Neural Information Processing Systems (NeurIPS)*, 2025. [1](#)
- [4] Junhao Cheng, Yuying Ge, Teng Wang, Yixiao Ge, Jing Liao, and Ying Shan. Video-holmes: Can mllm think like holmes for complex video reasoning? *arXiv preprint arXiv:2505.21374*, 2025. [7](#), [12](#), [13](#)
- [5] Zesen Cheng, Sicong Leng, Hang Zhang, Yifei Xin, Xin Li, Guanzheng Chen, Yongxin Zhu, Wenqi Zhang, Ziyang Luo, Deli Zhao, et al. Videollama 2: Advancing spatial-temporal modeling and audio understanding in video-lmms. *arXiv preprint arXiv:2406.07476*, 2024. [2](#)
- [6] Muzhi Dai, Chenxu Yang, and Qingyi Si. S-grpo: Early exit via reinforcement learning in reasoning models. In *Advances in Neural Information Processing Systems (NeurIPS)*, 2025. [1](#)
- [7] Jisheng Dang, Jingze Wu, Teng Wang, Xuanhui Lin, Nan-nan Zhu, Hongbo Chen, Wei-Shi Zheng, Meng Wang, and Tat-Seng Chua. Reinforcing video reasoning with focused thinking. *arXiv preprint arXiv:2505.24718*, 2025. [2](#), [6](#), [7](#)
- [8] Wenlong Deng, Yi Ren, Muchen Li, Danica J. Sutherland, Xiaoxiao Li, and Christos Thrampoulidis. On the effect of negative gradient in group relative deep reinforcement optimization. In *Advances in Neural Information Processing Systems (NeurIPS)*, 2025. [2](#)
- [9] Ding Ding, Zeqian Ju, Yichong Leng, Songxiang Liu, Tong Liu, Zeyu Shang, Kai Shen, Wei Song, Xu Tan, Heyi Tang, et al. Kimi-audio technical report. *arXiv preprint arXiv:2504.18425*, 2025. [6](#)
- [10] Kaixuan Fan, Kaituo Feng, Haoming Lyu, Dongzhan Zhou, and Xiangyu Yue. Sophiavrl1: Reinforcing mllms reasoning with thinking reward. *arXiv preprint arXiv:2505.17018*, 2025. [2](#)
- [11] Yue Fan, Xuehai He, Diji Yang, Kaizhi Zheng, Ching-Chen Kuo, Yuting Zheng, Sravana Jyothi Narayananaraju, Xinze Guan, and Xin Eric Wang. Grit: Teaching mllms to think with images. In *Advances in Neural Information Processing Systems (NeurIPS)*, 2025. [2](#), [12](#)
- [12] Kaituo Feng, Kaixiong Gong, Bohao Li, Zonghao Guo, Yibing Wang, Tianshuo Peng, Junfei Wu, Xiaoying Zhang, Benyou Wang, and Xiangyu Yue. Video-rl1: Reinforcing video reasoning in mllms. In *Advances in Neural Information Processing Systems (NeurIPS)*, 2025. [2](#), [5](#), [6](#)
- [13] Yunzhen Feng, Parag Jain, Anthony Hartshorn, Yaqi Duan, and Julia Kempe. Don't waste mistakes: Leveraging negative rl-groups via confidence reweighting. *arXiv preprint arXiv:2510.08696*, 2025. [1](#)
- [14] Chaoyou Fu, Haojia Lin, Zuwei Long, Yunhang Shen, Yuhang Dai, Meng Zhao, Yi-Fan Zhang, Shaoqi Dong, Yangze Li, Xiong Wang, et al. Vita: Towards open-source interactive omni multimodal llm. *arXiv preprint arXiv:2408.05211*, 2024. [2](#)
- [15] Chaoyou Fu, Yuhang Dai, Yongdong Luo, Lei Li, Shuhuai Ren, Renrui Zhang, Zihan Wang, Chenyu Zhou, Yunhang Shen, Mengdan Zhang, et al. Video-mme: The first-ever comprehensive evaluation benchmark of multi-modal llms in video analysis. In *Proceedings of the Computer Vision and Pattern Recognition Conference (CVPR)*, pages 24108–24118, 2025. [7](#)
- [16] Kaixiong Gong, Kaituo Feng, Bohao Li, Yibing Wang, Mofan Cheng, Shijia Yang, Jiaming Han, Benyou Wang, Yutong Bai, Zhuoran Yang, et al. Av-odyssey bench: Can your multimodal llms really understand audio-visual information? *arXiv preprint arXiv:2412.02611*, 2024. [7](#)
- [17] Daya Guo, Dejian Yang, Haowei Zhang, Junxiao Song, Ruoyu Zhang, Runxin Xu, Qihao Zhu, Shirong Ma, Peiyi Wang, Xiao Bi, et al. Deepseek-rl: Incentivizing reasoning capability in llms via reinforcement learning. *arXiv preprint arXiv:2501.12948*, 2025. [1](#), [2](#)
- [18] Jack Hong, Shilin Yan, Jiayin Cai, Xiaolong Jiang, Yao Hu, and Weidi Xie. Worldsense: Evaluating real-world omni-modal understanding for multimodal llms. *arXiv preprint arXiv:2502.04326*, 2025. [7](#)
- [19] Edward J Hu, Yelong Shen, Phillip Wallis, Zeyuan Allen-Zhu, Yuanzhi Li, Shean Wang, Lu Wang, Weizhu Chen, et al. Lora: Low-rank adaptation of large language models. In *International Conference on Learning Representations (ICLR)*, 2022. [6](#)
- [20] Qihan Huang, Weilong Dai, Jinlong Liu, Wanggui He, Hao Jiang, Mingli Song, Jingyuan Chen, Chang Yao, and Jie Song. Boosting mllm reasoning with text-debiased hint-grpo. In *Proceedings of the IEEE/CVF International Conference on Computer Vision (ICCV)*, 2025. [2](#), [4](#), [12](#)
- [21] Aaron Hurst, Adam Lerer, Adam P Goucher, Adam Perelman, Aditya Ramesh, Aidan Clark, AJ Ostrow, Akila Welihinda, Alan Hayes, Alec Radford, et al. Gpt-4o system card. *arXiv preprint arXiv:2410.21276*, 2024. [12](#), [18](#)

- [22] Md Mohaiminul Islam, Tushar Nagarajan, Huiyu Wang, Gedas Bertasius, and Lorenzo Torresani. Bimba: Selective-scan compression for long-range video question answering. In *Proceedings of the Computer Vision and Pattern Recognition Conference (CVPR)*, pages 29096–29107, 2025. 2
- [23] Yogesh Kulkarni and Pooyan Fazli. Videopasta: 7k preference pairs that matter for video-llm alignment. In *Empirical Methods in Natural Language Processing (EMNLP)*, 2025. 2
- [24] Yogesh Kulkarni and Pooyan Fazli. Videosavi: Self-aligned video language models without human supervision. In *Conference on Language Modeling (COLM)*, 2025. 2
- [25] Yuxiang Lai, Jike Zhong, Ming Li, Shitian Zhao, and Xiaofeng Yang. Med-r1: Reinforcement learning for generalizable medical reasoning in vision-language models. *arXiv preprint arXiv:2503.13939*, 2025. 2
- [26] Chaoyu Li, Eun Woo Im, and Pooyan Fazli. Vidhalluc: Evaluating temporal hallucinations in multimodal large language models for video understanding. In *Proceedings of the IEEE/CVF Conference on Computer Vision and Pattern Recognition (CVPR)*, pages 13723–13733, 2025. 1
- [27] Hongyu Li, Songhao Han, Yue Liao, Junfeng Luo, Jialin Gao, Shuicheng Yan, and Si Liu. Reinforcement learning tuning for videollms: Reward design and data efficiency. *arXiv preprint arXiv:2506.01908*, 2025. 12
- [28] Kunchang Li, Yali Wang, Yinan He, Yizhuo Li, Yi Wang, Yi Liu, Zun Wang, Jilan Xu, Guo Chen, Ping Luo, et al. Mvbench: A comprehensive multi-modal video understanding benchmark. In *Proceedings of the IEEE/CVF Conference on Computer Vision and Pattern Recognition (CVPR)*, pages 22195–22206, 2024. 7
- [29] Rui Li, Xiaohan Wang, Yuhui Zhang, Orr Zohar, Zeyu Wang, and Serena Yeung-Levy. Temporal preference optimization for long-form video understanding. *arXiv preprint arXiv:2501.13919*, 2025. 5
- [30] Siheng Li, Zhanhui Zhou, Wai Lam, Chao Yang, and Chaochao Lu. Repo: Replay-enhanced policy optimization. *arXiv preprint arXiv:2506.09340*, 2025. 1, 3, 4
- [31] Yizhi Li, Ge Zhang, Yinghao Ma, Ruibin Yuan, Kang Zhu, Hangyu Guo, Yiming Liang, Jiaheng Liu, Zekun Wang, Jian Yang, et al. Omnibench: Towards the future of universal omni-language models. In *Advances in Neural Information Processing Systems (NeurIPS)*, 2024. 7
- [32] Yunxin Li, Xinyu Chen, Zitao Li, Zhenyu Liu, Longyue Wang, Wenhan Luo, Baotian Hu, and Min Zhang. Veripo: Cultivating long reasoning in video-llms via verifier-guided iterative policy optimization. *arXiv preprint arXiv:2505.19000*, 2025. 12
- [33] Zichen Liu, Changyu Chen, Wenjun Li, Penghui Qi, Tianyu Pang, Chao Du, Wee Sun Lee, and Min Lin. Understanding r1-zero-like training: A critical perspective. In *Conference on Language Modeling (COLM)*, 2025. 1
- [34] Zuyan Liu, Yuhao Dong, Jiahui Wang, Ziwei Liu, Winston Hu, Jiwen Lu, and Yongming Rao. Ola: Pushing the frontiers of omni-modal language model. *arXiv preprint arXiv:2502.04328*, 2025. 5, 6
- [35] Ziyu Liu, Zeyi Sun, Yuhang Zang, Xiaoyi Dong, Yuhang Cao, Haodong Duan, Duhua Lin, and Jiaqi Wang. Visual-rft: Visual reinforcement fine-tuning. In *Proceedings of the IEEE/CVF International Conference on Computer Vision (ICCV)*, 2025. 1
- [36] Lidong Lu, Guo Chen, Zhiqi Li, Yicheng Liu, and Tong Lu. Av-reasoner: Improving and benchmarking clue-grounded audio-visual counting for mllms. *arXiv preprint arXiv:2506.05328*, 2025. 1, 2, 5, 6, 7, 12
- [37] Desen Meng, Rui Huang, Zhilin Dai, Xinhao Li, Yifan Xu, Jun Zhang, Zhenpeng Huang, Meng Zhang, Lingshu Zhang, Yi Liu, et al. Videocap-r1: Enhancing mllms for video captioning via structured thinking. *arXiv preprint arXiv:2506.01725*, 2025. 2
- [38] Prasanna Parthasarathi, Mathieu Reymond, Boxing Chen, Yufei Cui, and Sarah Chandar. Grpo-λ: Credit assignment improves llm reasoning. *arXiv preprint arXiv:2510.00194*, 2025. 4
- [39] Rafael Rafailov, Archit Sharma, Eric Mitchell, Christopher D Manning, Stefano Ermon, and Chelsea Finn. Direct preference optimization: Your language model is secretly a reward model. In *Advances in Neural Information Processing Systems (NeurIPS)*, 2023. 2
- [40] Soumya Rani Samineni, Durgesh Kalwar, Karthik Valmeekam, Kaya Stechly, and Subbarao Kambhampati. Rl in name only? analyzing the structural assumptions in rl post-training for llms. *arXiv preprint arXiv:2505.13697*, 2025. 2
- [41] Gabriel Sarch, Snigdha Saha, Naitik Khandelwal, Ayush Jain, Michael J. Tarr, Aviral Kumar, and Katerina Fragkiadaki. Grounded reinforcement learning for visual reasoning. In *Advances in Neural Information Processing Systems (NeurIPS)*, 2025. 12
- [42] Pritam Sarkar and Ali Etemad. Self-alignment of large video language models with refined regularized preference optimization. In *Advances in Neural Information Processing Systems (NeurIPS)*, 2025. 2
- [43] Ziyao Shangguan, Chuhan Li, Yuxuan Ding, Yanan Zheng, Yilun Zhao, Tesca Fitzgerald, and Arman Cohan. Tomato: Assessing visual temporal reasoning capabilities in multimodal foundation models. In *Proceedings of the International Conference on Learning Representations (ICLR)*, 2025. 7
- [44] Guangming Sheng, Chi Zhang, Zilingfeng Ye, Xibin Wu, Wang Zhang, Ru Zhang, Yanghua Peng, Haibin Lin, and Chuan Wu. Hybridflow: A flexible and efficient rlhf framework. In *Proceedings of the Twentieth European Conference on Computer Systems (EuroSys)*, pages 1279–1297, 2025. 1
- [45] Guangzhi Sun, Yudong Yang, Jimin Zhuang, Changli Tang, Yixuan Li, Wei Li, Zejun Ma, and Chao Zhang. video-salmonn-o1: Reasoning-enhanced audio-visual large language model. In *International Conference on Machine Learning (ICML)*, 2025. 2
- [46] Yunlong Tang, Daiki Shimada, Jing Bi, Mingqian Feng, Hang Hua, and Chenliang Xu. Empowering llms with pseudo-untrimmed videos for audio-visual temporal understanding. In *Proceedings of the AAAI Conference on Artificial Intelligence (AAAI)*, pages 7293–7301, 2025. 2
- [47] Yapeng Tian, Jing Shi, Bochen Li, Zhiyao Duan, and Chenliang Xu. Audio-visual event localization in unconstrained

- videos. In *Proceedings of the European Conference on Computer Vision (ECCV)*, pages 247–263, 2018. 5
- [48] Zhongwei Wan, Zhihao Dou, Che Liu, Yu Zhang, Dongfei Cui, Qinjian Zhao, Hui Shen, Jing Xiong, Yi Xin, Yifan Jiang, Chaofan Tao, Yangfan He, Mi Zhang, and Shen Yan. Srp0: Enhancing multimodal llm reasoning via reflection-aware reinforcement learning. In *Advances in Neural Information Processing Systems (NeurIPS)*, 2025. 12
- [49] Haozhe Wang, Chao Qu, Zuming Huang, Wei Chu, Fangzhen Lin, and Wenhui Chen. Vl-rethinker: Incentivizing self-reflection of vision-language models with reinforcement learning. In *Advances in Neural Information Processing Systems (NeurIPS)*, 2025. 1, 3, 4
- [50] Qi Wang, Yanrui Yu, Ye Yuan, Rui Mao, and Tianfei Zhou. Videorf: Incentivizing video reasoning capability in mllms via reinforced fine-tuning. In *Advances in Neural Information Processing Systems (NeurIPS)*, 2025. 1, 6
- [51] Song Wang, Gongfan Fang, Lingdong Kong, Xiangtai Li, Jianyun Xu, Sheng Yang, Qiang Li, Jianke Zhu, and Xinchao Wang. Pixelthink: Towards efficient chain-of-pixel reasoning. *arXiv preprint arXiv:2505.23727*, 2025. 12
- [52] Weihan Wang, Zehai He, Wenyi Hong, Yean Cheng, Xiaohan Zhang, Ji Qi, Xiaotao Gu, Shiyu Huang, Bin Xu, Yuxiao Dong, Ming Ding, and Jie Tang. Lvbench: An extreme long video understanding benchmark. In *Proceedings of the IEEE/CVF International Conference on Computer Vision (ICCV)*, 2025. 7
- [53] Zhenhai long Wang, Xuehang Guo, Sofia Stoica, Haiyang Xu, Hongru Wang, Hyeonjeong Ha, Xiusi Chen, Yangyi Chen, Ming Yan, Fei Huang, et al. Perception-aware policy optimization for multimodal reasoning. *arXiv preprint arXiv:2507.06448*, 2025. 2, 12
- [54] Ziyang Wang, Jaehong Yoon, Shoubin Yu, Md Mohaiminul Islam, Gedas Bertasius, and Mohit Bansal. Video-rts: Rethinking reinforcement learning and test-time scaling for efficient and enhanced video reasoning. In *Empirical Methods in Natural Language Processing (EMNLP)*, 2025. 1, 12
- [55] Lai Wei, Yuting Li, Kaipeng Zheng, Chen Wang, Yue Wang, Linghe Kong, Lichao Sun, and Weiran Huang. Advancing multimodal reasoning via reinforcement learning with cold start. *arXiv preprint arXiv:2505.22334*, 2025. 12
- [56] Wenyi Xiao, Leilei Gan, Weilong Dai, Wanggui He, Ziwei Huang, Haoyuan Li, Fangxun Shu, Zhelun Yu, Peng Zhang, Hao Jiang, and Fei Wu. Fast-slow thinking for large vision-language model reasoning. In *Advances in Neural Information Processing Systems (NeurIPS)*, 2025. 12
- [57] Guofu Xie, Yunsheng Shi, Hongtao Tian, Ting Yao, and Xiao Zhang. Capo: Towards enhancing llm reasoning through verifiable generative credit assignment. *arXiv preprint arXiv:2508.02298*, 2025. 4
- [58] Zhenghao Xing, Xiaowei Hu, Chi-Wing Fu, Wenhui Wang, Jifeng Dai, and Pheng-Ann Heng. Echoink-r1: Exploring audio-visual reasoning in multimodal llms via reinforcement learning. *arXiv preprint arXiv:2505.04623*, 2025. 6, 12
- [59] Jin Xu, Zhifang Guo, Jinzheng He, Hangrui Hu, Ting He, Shuai Bai, Keqin Chen, Jialin Wang, Yang Fan, Kai Dang, et al. Qwen2. 5-omni technical report. *arXiv preprint arXiv:2503.20215*, 2025. 5, 6, 16
- [60] Pinci Yang, Xin Wang, Xuguang Duan, Hong Chen, Runze Hou, Cong Jin, and Wenwu Zhu. Avqa: A dataset for audio-visual question answering on videos. In *Proceedings of the ACM International Conference on Multimedia (MM)*, 2022. 5
- [61] Qilang Ye, Zitong Yu, Rui Shao, Xinyu Xie, Philip Torr, and Xiaochun Cao. Cat: Enhancing multimodal large language model to answer questions in dynamic audio-visual scenarios. In *European Conference on Computer Vision (ECCV)*, pages 146–164, 2024. 2
- [62] Jiaxing Zhao, Qize Yang, Yixing Peng, Detao Bai, Shimin Yao, Boyuan Sun, Xiang Chen, Shenghao Fu, Xihan Wei, Liefeng Bo, et al. Humanomni: A large vision-speech language model for human-centric video understanding. *arXiv preprint arXiv:2501.15111*, 2025. 2, 6, 7, 12
- [63] Yuze Zhao, Jintao Huang, Jinghan Hu, Xingjun Wang, Yunlin Mao, Daoze Zhang, Zeyinzi Jiang, Zhikai Wu, Baole Ai, Ang Wang, et al. Swift: a scalable lightweight infrastructure for fine-tuning. In *Proceedings of the AAAI Conference on Artificial Intelligence (AAAI)*, pages 29733–29735, 2025. 6
- [64] Yilun Zhao, Haowei Zhang, Lujing Xie, Tongyan Hu, Guo Gan, Yitao Long, Zhiyuan Hu, Weiyuan Chen, Chuhan Li, Zhijian Xu, Chengye Wang, Ziyao Shangguan, Zhenwen Liang, Yixin Liu, Chen Zhao, and Arman Cohan. Mmvu: Measuring expert-level multi-discipline video understanding. In *Proceedings of the Computer Vision and Pattern Recognition Conference (CVPR)*, pages 8475–8489, 2025. 7
- [65] Hao Zhong, Muzhi Zhu, Zongze Du, Zheng Huang, Canyu Zhao, Mingyu Liu, Wen Wang, Hao Chen, and Chunhua Shen. Omni-r1: Reinforcement learning for omnimodal reasoning via two-system collaboration. In *Advances in Neural Information Processing Systems (NeurIPS)*, 2025. 1, 2, 6, 12
- [66] Jinxing Zhou, Jianyuan Wang, Jiayi Zhang, Weixuan Sun, Jing Zhang, Stan Birchfield, Dan Guo, Lingpeng Kong, Meng Wang, and Yiran Zhong. Audio-visual segmentation. In *European Conference on Computer Vision (ECCV)*, pages 386–403, 2022. 5
- [67] Ziwei Zhou, Rui Wang, and Zuxuan Wu. Daily-omni: Towards audio-visual reasoning with temporal alignment across modalities. *arXiv preprint arXiv:2505.17862*, 2025. 7
- [68] Jinguo Zhu, Weiyun Wang, Zhe Chen, Zhaoyang Liu, Shenglong Ye, Lixin Gu, Hao Tian, Yuchen Duan, Weijie Su, Jie Shao, et al. Internvl3: Exploring advanced training and test-time recipes for open-source multimodal models. *arXiv preprint arXiv:2504.10479*, 2025. 2, 5, 6

Appendix

A. GRPO for Multimodal Reasoning

Recent works increasingly use RL methods, particularly GRPO [48, 53, 56], introducing new challenges related to training efficiency and stability. Wei et al. propose a “cold start” strategy via Supervised Fine-Tuning (SFT) before RL [55], while other approaches improve data efficiency through direct RL with test-time scaling [54]. Concurrent advances enhance GRPO through curriculum learning [36], variance-aware data selection [27], hint-based guidance for difficult samples [20], and combining GRPO and DPO [32]. Key limitations remain, including the “overthinking” issue, addressed by regulating reasoning length [51, 56], and perception errors mitigated via grounded reasoning approaches [11, 41] and new RL objectives such as PAPO’s Implicit Perception Loss [53].

Audio-visual reasoning that incorporates audio often involves trade-offs between temporal coverage and spatial resolution. These challenges have been addressed through two-system architectures [65], explicit contextual rewards [62], and task-specific improvements [36, 58]. AVATAR introduces a unified framework that integrates a stratified replay buffer for curriculum learning with Temporal Advantage Shaping (TAS) for credit assignment. This approach improves reasoning and grounding within a single model, eliminating the need for two-system architectures [65] or explicit visual coordinate generation [41].

B. Ablation Studies

RQ1: Is TAS a principled, critic-free credit assignment strategy? We argue that TAS is a *data-driven approximation* that directly exploits the strong structural prior learned during our SFT (Stage 0). The SFT phase trains the model to generate reasoning in a predictable *planning-evidence-synthesis* structure.

To validate this, we empirically analyzed the positional distribution of “critical reasoning steps” (tokens with the highest causal impact on the final answer) from 50,000 samples in our SFT dataset. This analysis was verified using GPT-4o [21] (Prompt provided in Figure 12) to identify the most critical reasoning step for each sample. Figure 6 shows this empirical distribution (blue bars), which is distinctly parabolic-shaped: critical tokens cluster at the sequence start (*planning*, $\tilde{t} \in [0, 0.2]$) and end (*synthesis*, $\tilde{t} \in [0.8, 1.0]$), while intermediate *evidence* gathering tokens are far less critical.

This empirical result validates that TAS’s parabolic function (orange line) is a *principled, low-cost approximation of the true importance distribution* in our data. This design is a key advantage: it achieves effective temporal credit assignment by leveraging the *known structure* of the reasoning,

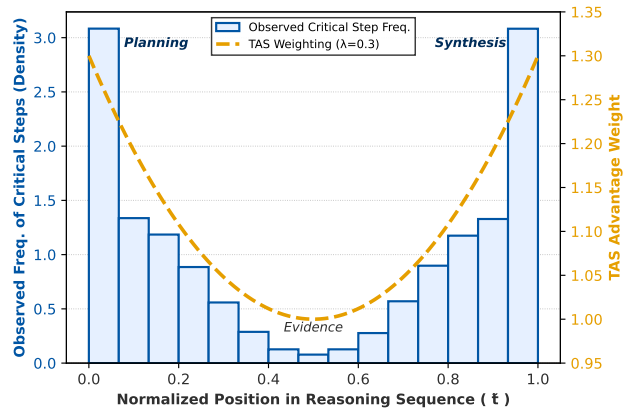


Figure 6. **TAS is a Data-Driven Approximation.** We empirically analyze the distribution of “critical reasoning steps” from our SFT data. The resulting U-shaped histogram (blue bars) shows that important tokens cluster at the *planning* and *synthesis* phases. TAS’s parabolic function (orange, $\lambda_{TAS}=0.3$) is a simple, critic-free function that directly approximates this observed data.

bypassing the need to train a complex, unstable, and high-variance value function or critic. Standard GRPO’s uniform credit assignment dilutes the learning signal by applying A_i to all tokens equally. By modulating this with our data-driven weights $w_{i,t}$, the shaped advantage $A_{i,t}^{TAS}$ focuses the policy gradient onto the tokens most critical for a correct outcome, providing a stable and efficient learning signal.

RQ2: Does TAS empirically focus the learning signal in practice? Figure 6 established why a parabolic-shaped function is the correct model: the problem (critical steps) is empirically parabolic-shaped. Here, we validate that our solution (the learning signal) successfully adopts this parabolic-shape in practice. We performed an analysis over the Video-Holmes [4] benchmark, calculating the average per-token loss (the learning signal) against its normalized position. Figure 8 shows the result. The Baseline GRPO (blue dashed line) exhibits a relatively flat loss distribution. This is the empirical evidence of *uniform credit assignment*: the learning signal is diluted by being applied unfocused and equally to all tokens, regardless of their importance. In contrast, AVATAR w/ TAS (orange solid line) demonstrates a clear parabolic-shaped loss profile. The shaped advantage $A_{i,t}^{TAS}$ *amplifies the learning signal* at the critical *planning* ($\tilde{t} \in [0, 0.2]$) and *synthesis* ($\tilde{t} \in [0.8, 1.0]$) phases. This proves TAS is a functioning mechanism: it forces the optimizer to learn most aggressively from errors in the most important parts of the reasoning chain.

RQ3: What is the impact of the on-policy/off-policy sample ratio? To determine the optimal balance between on-policy and off-policy data, we analyze performance across different sample ratios within a fixed group size of eight (Figure 7). We observe a consistent trend across all bench-

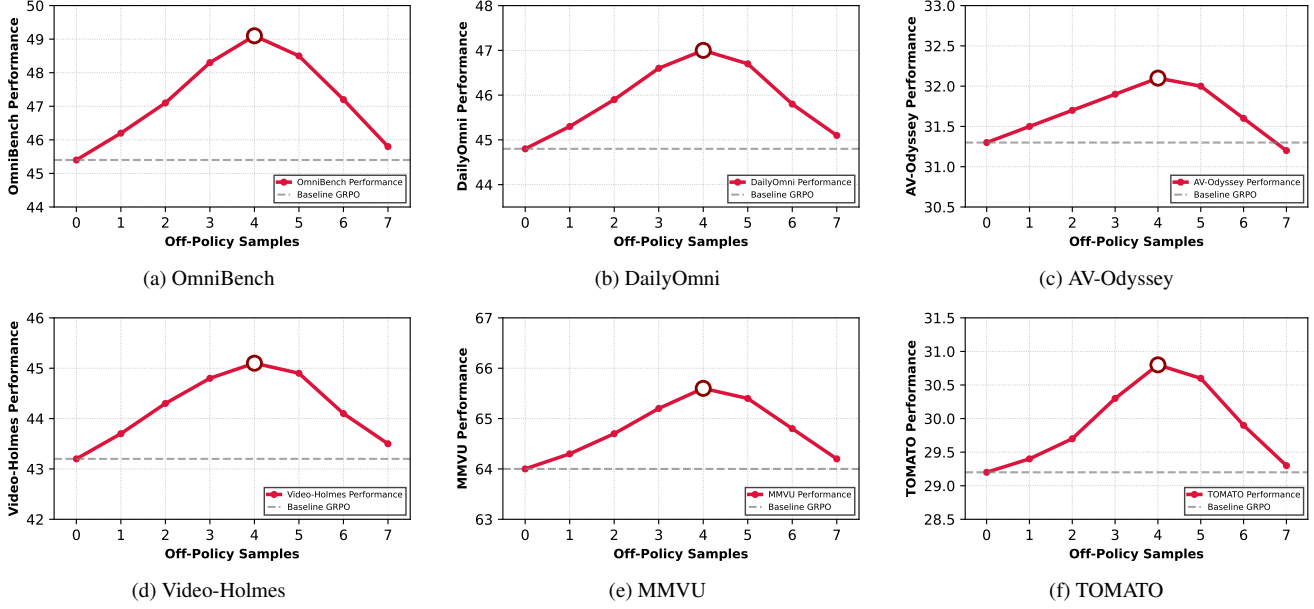


Figure 7. **Performance vs. on-policy/off-policy sample ratio across six benchmarks.** AVATAR achieves optimal performance with 4-4 split (4 on-policy, 4 off-policy samples), demonstrating that balanced mixing prevents both policy drift from excessive off-policy data and sample inefficiency from pure on-policy training.

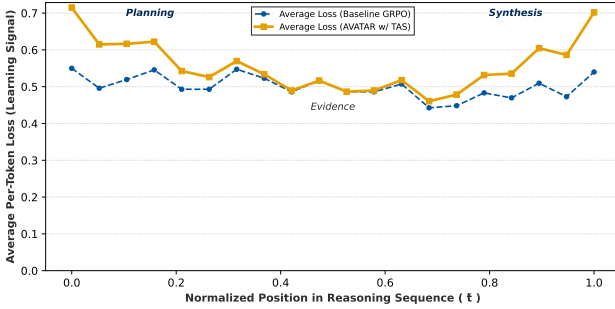


Figure 8. **TAS Empirically Focuses the Learning Signal.** We plot the average per-token loss (the learning signal) vs. normalized position across the Video-Holmes [4] benchmark. The **Baseline GRPO** (blue dashed line) shows a flat, unfocused signal, indicative of **uniform credit assignment**. AVATAR w/ TAS (orange solid line) successfully focuses the learning signal, amplifying it on the critical *planning* and *synthesis* phases.

marks: performance peaks when using a balanced 4-4 split (4 on-policy, 4 off-policy samples). Using fewer off-policy samples (0-3) fails to fully mitigate the data inefficiency of a purely on-policy approach. On the other hand, over-reliance on off-policy samples (5-7) degrades performance due to instability, as the policy drifts too far from the older, “stale” data in the replay buffer. The 4-4 split therefore represents an empirical sweet spot for AVATAR, maximizing the data efficiency gains of our off-policy architecture while maintaining the training stability necessary for effective learning.

Table 7. **Ablation on key reasoning tasks from the WorldSense benchmark.** Halluc: Hallucination, TP: Temporal Prediction, AC: Audio Change

Config	Halluc	TP	AC
Baseline GRPO	35.6	53.6	32.5
AVATAR w/o Off-Policy	40.1 (+4.5)	54.8 (+1.2)	34.1 (+1.6)
AVATAR w/o TAS	48.9 (+13.3)	56.1 (+2.5)	35.8 (+3.3)
AVATAR (Full)	51.2 (+15.6)	57.2 (+3.6)	37.3 (+4.8)

RQ4: How do AVATAR’s components impact audio-visual reasoning? The impact is evident on reasoning tasks from the WorldSense benchmark (Table 7). The highest improvement is on the *Hallucination* task, a gain primarily driven by our off-policy architecture, which builds a more robust and grounded model by forcing repeated engagement with difficult samples from the hard tier. The effect of TAS is most clear on tasks requiring temporal logic, such as *Temporal Prediction*, which involves forecasting future events, and *Audio Change*, which requires identifying discrete shifts in the audio stream. The U-shaped weighting of TAS is uniquely suited for these problems, by modifying credit for initial tokens, it forces accurate grounding of the video’s initial state, while modifying credit for final tokens rewards correct synthesis of how that state evolved over time.

RQ5: Impact of λ_{TAS} on Learning Stability. As illustrated in Figure 9, model performance exhibits a clear three-phase

Table 8. **Ablation studies on our reward strategy across three training stages.** Stage 1 uses R_{acc} and R_{format} for basic accuracy and format compliance. Stage 2 adds R_{self} (majority vote consensus) to the existing rewards, enabling consistency learning. Stage 3 incorporates R_{judge} (stepwise VLM evaluation) alongside all previous rewards, providing detailed reasoning feedback. VCRS maintains stable advantage baselines through moving averages, preventing vanishing advantages. Each cumulative addition demonstrates clear performance gains, with largest improvements on reasoning-heavy benchmarks (Video-Holmes: +4.5, MMVU: +5.4) where structured feedback proves most beneficial.

Ablation Configuration		Audio-Visual Benchmarks			Video Reasoning Benchmarks		
Group	Setting	OmniBench	DailyOmni	AV-Odyssey	Video-Holmes	MMVU	TOMATO
	Baseline Qwen2.5 Omni	44.2	44.0	29.8	40.6	60.2	29.0
Reward Suite	$R_{\text{acc}} + R_{\text{format}}$	46.8 (+2.6)	45.2 (+1.2)	30.1 (+0.3)	42.3 (+1.7)	62.1 (+1.9)	28.9 (-0.1)
	$R_{\text{acc}} + R_{\text{format}} + R_{\text{self}}$	47.5 (+3.3)	45.8 (+1.8)	30.7 (+0.9)	43.1 (+2.5)	63.4 (+3.2)	29.4 (+0.4)
	$R_{\text{acc}} + R_{\text{format}} + R_{\text{self}} + R_{\text{judge}}$	48.3 (+4.1)	46.4 (+2.4)	31.4 (+1.6)	44.2 (+3.6)	64.7 (+4.5)	30.1 (+1.1)
	$R_{\text{acc}} + R_{\text{format}} + R_{\text{self}} + R_{\text{judge}} + \text{VCRS}$	49.1 (+4.9)	47.0 (+3.0)	32.1 (+2.3)	45.1 (+4.5)	65.6 (+5.4)	30.8 (+1.8)

trend with respect to λ_{TAS} . At low values ($\lambda_{\text{TAS}} < 0.1$), the reward shaping effect is weak, leading to slower convergence and unstable gains. As λ_{TAS} increases to a moderate level ($\lambda_{\text{TAS}} \approx 0.3$), performance peaks across both audio-visual and video reasoning benchmarks, reflecting a balanced trade-off between stability and exploration. However, at higher values ($\lambda_{\text{TAS}} > 1.0$), the model becomes over-regularized, reducing adaptability and leading to gradual accuracy decline.

RQ6: How do isolating rewards impact performance?

Table 8 shows the cumulative impact of each reward component in AVATAR’s training pipeline. The baseline, which includes only accuracy and format rewards, offers limited learning signals, especially on complex reasoning tasks such as Video-Holmes and MMVU, where binary feedback proves insufficient. Introducing self-rewarding (R_{self}) in Stage 2 enables consensus-based learning from the model’s own outputs, yielding moderate improvements on audio-visual tasks that benefit from internal consistency signals (e.g., +0.7 on OmniBench, +1.3 on MMVU). Adding the stepwise judge reward (R_{judge}) in Stage 3 results in larger gains by assessing intermediate reasoning steps, particularly enhancing performance on fine-grained localization benchmarks (e.g., +0.8 on OmniBench, +1.3 on MMVU). Finally, incorporating VCRS further stabilizes training by maintaining non-zero advantage baselines via moving averages, allowing the full reward setup to achieve the highest observed performance (e.g., +0.8 on OmniBench, +0.9 on MMVU).

RQ7: How do training dynamics differ across benchmarks? The training curves in Figure 10 reveal distinct learning patterns that directly validate our core contributions. Baseline GRPO shows a consistent decline across all benchmarks due to the vanishing advantage problem: when encountering difficult samples where all responses receive similar rewards, the learning signal collapses to zero, stalling further learning. As a result, GRPO quickly plateaus and fails to move beyond solving only the simplest queries.

In contrast, AVATAR shows a *dip-and-recovery pattern* that

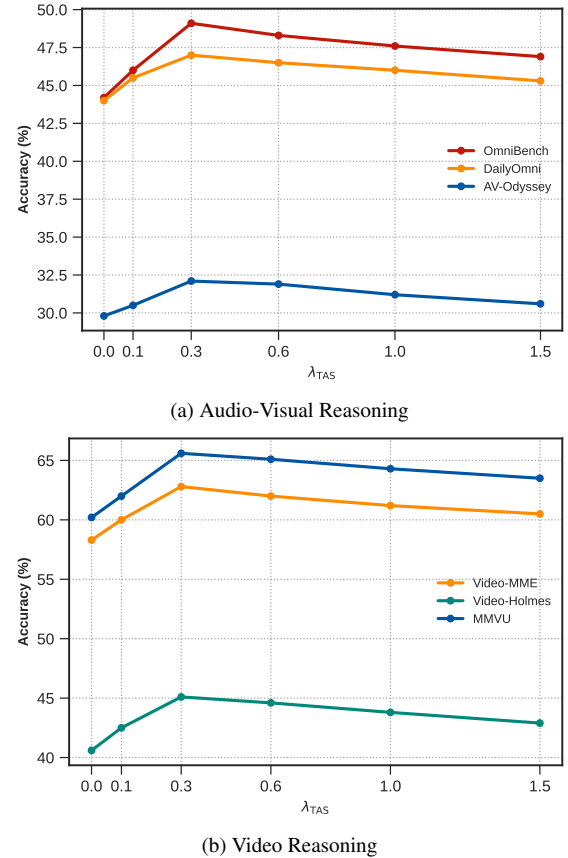


Figure 9. **Performance variation with TAS weighting (λ_{TAS}).** Both (a) **Audio-Visual** and (b) **Video Reasoning** benchmarks peak around $\lambda_{\text{TAS}}=0.3$, showing improved stability and reward shaping before slight decline at higher values.

reflects the interplay of its key components. The initial drop in performance, especially on challenging benchmarks like OmniBench, Video-Holmes, and MMVU, occurs when the stratified replay buffer transitions from easy to hard sam-

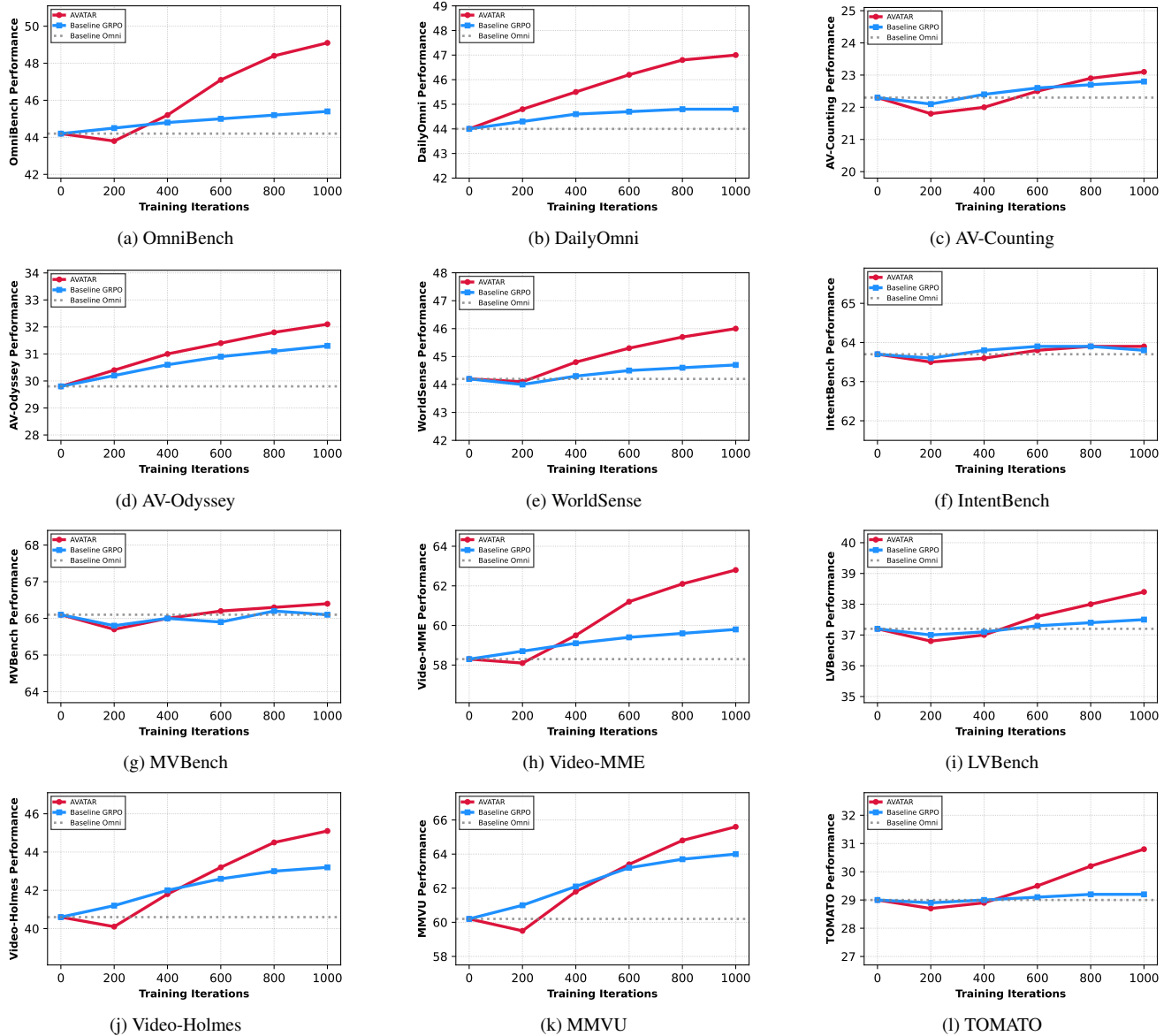


Figure 10. **Training curves across audio-visual and video reasoning benchmarks. AVATAR demonstrates superior sample efficiency and final performance**, particularly on challenging reasoning tasks. AVATAR’s initial dip, followed by a strong recovery, validates the effectiveness of our off-policy architecture and TAS for credit assignment.

plexes, exposing the model to its most difficult failures. This performance dip would persist without TAS; however, the U-shaped temporal weighting in TAS provides focused learning signals that extract meaningful gradients from these difficult examples. By emphasizing the planning and synthesis phases that uniform credit assignment would dilute, TAS enables recovery and subsequent improvement. The model’s rebound and higher final performance confirm that our off-policy architecture transforms early failure into learning opportunities through repeated exposure, while TAS ensures each replayed experience yields maximum value. Notably,

these gains emerge within just 1000 iterations, underscoring AVATAR’s superior sample efficiency and training effectiveness.

RQ8: What is impact of replay buffer size? The total size of the replay buffer introduces a critical trade-off between sample diversity and data staleness. A larger buffer holds a more diverse set of past experiences, especially difficult samples, which can improve generalization. However, a buffer that is too large increases the risk of sampling “stale” data generated by a much older policy, which can destabilize the off-policy learning. This trade-off is empirically validated in

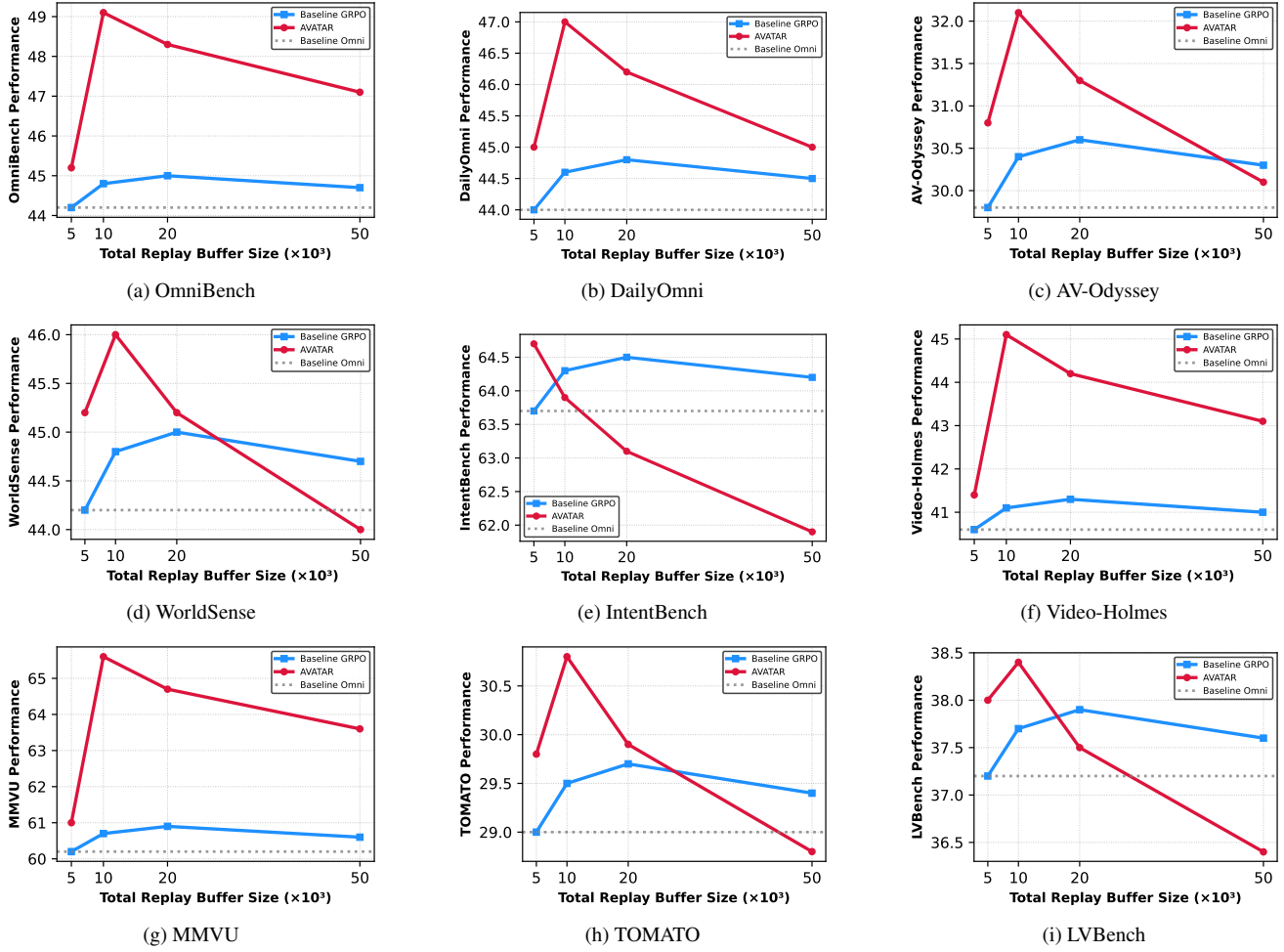


Figure 11. **Ablation on total replay buffer capacity across audio-visual and video reasoning benchmarks.** Performance peaks consistently at around **10k buffer size**, balancing diversity and staleness in experience replay. **AVATAR achieves higher and more stable gains** than GRPO across all tasks, validating its curriculum-based replay and TAS advantage shaping as critical for robust multimodal learning.

Figure 11. Across all benchmarks, performance consistently peaks at an optimal capacity of 10k samples. Below this size, performance suffers from a lack of diversity; beyond this point, performance degrades as the negative impact of data staleness begins to outweigh the benefits of diversity.

RQ9: Does AVATAR generalize to smaller models? To evaluate the generalizability of our approach across different model scales, we conduct experiments with a 3B parameter version of the base Qwen2.5 Omni [59] model. Tables 9 and 10 demonstrate that AVATAR consistently outperforms both the baseline and on-policy GRPO across all benchmarks, achieving notable improvements of +3.4 on OmniBench, +2.9 on Video-Holmes, and +2.8 on MMVU. These results validate that AVATAR’s core components, the stratified replay buffer and TAS, effectively enhance multimodal reasoning capabilities regardless of language model

scale. The consistent performance patterns across different model sizes further confirm that our off-policy architecture is broadly applicable, with particularly strong benefits observed on complex reasoning tasks where AVATAR’s targeted learning signals prove most impactful for guiding model improvement.

B.1. Prompt Templates

To support AVATAR’s training pipeline, we use two prompt templates for different components of our framework. The *hint generation prompt* (Figure 13) is used by our stratified replay buffer’s hint mechanism when the policy becomes stuck in local optima on challenging samples. This prompt instructs a teacher model to generate strategic hints without revealing the final answer, helping the policy escape stagnation while maintaining the learning challenge. The

Table 9. **Audio-visual benchmarks: 3B model comparison.** AVATAR 3B consistently outperforms both the baseline 3B Omni and baseline GRPO across all benchmarks, achieving improvements of +3.4 on OmniBench and +2.6 on AV-Odyssey. The results demonstrate that our off-policy architecture and TAS effectively enhance multimodal reasoning capabilities even with smaller model scales, validating the broad applicability of our approach. Performance improvements over baseline 3B Omni are shown in green.

Audio-Visual Benchmarks						
Model	OmniBench	DailyOmni	AV-Counting	AV-Odyssey	WorldSense	IntentBench
Baseline 3B Omni	42.4	42.9	19.7	27.2	35.2	59.7
Baseline GRPO	43.1 (+0.7)	43.4 (+0.5)	20.0 (+0.3)	28.5 (+1.3)	35.8 (+0.6)	59.9 (+0.2)
AVATAR 3B	45.8 (+3.4)	44.7 (+1.8)	20.9 (+1.2)	29.8 (+2.6)	37.1 (+1.9)	60.5 (+0.8)

Table 10. **Video understanding and reasoning benchmarks: 3B model comparison.** AVATAR 3B demonstrates superior performance across both general video understanding and complex reasoning tasks, with particularly strong gains on reasoning-heavy benchmarks like Video-Holmes (+2.9) and MMVU (+2.8). The consistent improvements over baseline GRPO highlight how our stratified replay buffer and TAS enhance learning efficiency even with reduced model capacity, confirming that our framework’s benefits scale effectively across different model sizes. Performance improvements over baseline 3B Omni are shown in green.

Model	General Video Understanding			Video Reasoning		
	MVBench	Video-MME	LVBench	Video-Holmes	MMVU	TOMATO
Baseline 3B Omni	59.2	57.6	34.3	39.2	62.0	27.0
Baseline GRPO	59.8 (+0.6)	58.1 (+0.5)	34.7 (+0.4)	40.8 (+1.6)	63.2 (+1.2)	27.3 (+0.3)
AVATAR 3B	61.2 (+2.0)	59.9 (+2.3)	35.8 (+1.5)	42.1 (+2.9)	64.8 (+2.8)	28.4 (+1.4)

audio-visual localization judge prompt (Figure 14) helps our stepwise reasoning judge in Stage 3 training by providing granular evaluation criteria across four dimensions: grounding of audio cues, identification of visual objects, spatial localization accuracy, and caption correctness. This offers detailed feedback on cross-modal reasoning quality rather than binary success/failure signals.

B.2. Qualitative Analysis

Figure 15 illustrates the qualitative differences between baseline GRPO and AVATAR on audio-visual reasoning tasks. AVATAR demonstrates *superior cross-modal integration* by linking visual cues (“tense expression, his eyes darting around”) with audio analysis (“hurried and tense tone when he speaks”), while baseline GRPO makes *disconnected observations*, such as “He looks worried which indicates stress” without linking modalities. The responses highlight the effectiveness of TAS, evident in the model’s ability to *plan* by establishing comprehensive scene context, focus on relevant cues while avoiding *redundant pattern matching* (e.g., “Black clothing often symbolizes negativity”), and *synthesize* complex emotional dynamics rather than relying on *surface-level assumptions* (“something bad might be happening”). AVATAR also shows *improved temporal reasoning* by tracking emotional progression (“tone shifting from calm to

anxious”) and *enhanced contextual understanding* through precise dialogue interpretation (“Sorry, I have a train to catch” indicating abrupt departure). In contrast, baseline GRPO tends to fall back on *generic genre classifications* (“suggests a thriller or drama genre”). These qualitative differences validate our framework’s ability to enhance multimodal reasoning quality through targeted credit assignment and structured learning signals.

GPT-4o Prompt for Critical Step Analysis (TAS Justification)

You are an expert evaluator of multimodal reasoning. Your task is to analyze a Chain-of-Thought (CoT) trace and identify the **single most critical reasoning step**. This is the specific step, phrase, or sentence that, if removed or incorrect, would cause the entire reasoning chain to fail.

After identifying this single critical step, you must classify it into one of the following three categories:

- **PLANNING**: The step involves strategy, problem decomposition, or forming an initial hypothesis. (e.g., “I need to first locate the sound, then identify the object.”)
- **EVIDENCE**: The step involves observing unimodal or multimodal facts from the video or audio. (e.g., “The video shows a man wearing a red hat.”, “The audio caption mentions ‘clapping’.”)
- **SYNTHESIS**: The step involves combining multiple pieces of evidence, performing a final calculation, or forming the final conclusion. (e.g., “Since the man is running and the music is fast, the scene is urgent.”, “Count: 3 objects.”)

You will be given the user's query and the model's reasoning trace.

[User Query]: {The original question posed to the model.}

[Reasoning CoT]: {The full reasoning trace expected from the model, contained within <think>...</think> tags.}

Your Task: Analyze the [Reasoning CoT] and identify the single most critical step. Then, classify it.

Constraints:

- You **must** output a single, valid JSON object.
- The JSON object must contain exactly two keys: “category” and “critical_step”.
- The value for “category” **must** be one of: PLANNING, EVIDENCE, or SYNTHESIS.
- The value for “critical_step” **must** be the exact text of the reasoning step you identified.

Example 1 (Planning):

```
[User Query]: How many moving rubber objects are there when the video ends?  
[Reasoning CoT]: <think>  
1. I need to identify objects that are 'rubber'.  
2. I need to check if they are 'moving'.  
3. I must check this at the 'end' of the video.  
4. Then I will count them.  
5. Green cylinder is rubber. It moves from collisions. At the end, it is moving.  
6. Count: 1 moving rubber object.  
</think>  
  
Output:  
{'category': 'PLANNING', 'critical_step': '1. I need to identify objects  
that are 'rubber'. 2. I need to check if they are 'moving'. 3. I must  
check this at the 'end' of the video.'}
```

Example 2 (Synthesis):

```
[User Query]: What is the audience's reaction during the woman's speech?  
[Reasoning CoT]: <think>  
1. The audio caption says 'A crowd cheers and a woman speaks'.  
2. The video shows a woman at a podium and an audience.  
3. The audio cue 'cheers' corresponds to the visual 'audience'.  
4. 'Cheers' are a positive reaction.  
5. Therefore, the audience reaction is positive.  
</think>  
  
Output:  
{'category': 'SYNTHESIS', 'critical_step': '5. Therefore, the audience  
reaction is positive.'}
```

Figure 12. The GPT-4o [21] prompt template used to identify and categorize the critical reasoning step from 50,000 SFT samples.

Hint Generation Prompt for Hard Samples

You are an expert AI tutor. Your task is to provide a concise, strategic hint to a student model that is struggling with a difficult audio-visual reasoning problem. The student model is consistently failing this problem and has stopped exploring new reasoning paths. Your hint should guide it out of a local minimum without solving the problem for it. Given the following full problem context:

[User Query]: {The original question posed to the student model.}

[Audio Caption]: {A transcript of the relevant audio from the video clip.}

[Video Context]: {The full video clip associated with the query.}

[Ground Truth Answer]: {The correct final answer to the query.}

Your Task: Based on the full context and the ground truth, generate a single, short sentence that provides a high-level strategy for how to approach the problem.

Constraints:

- **DO NOT** reveal or allude to the final answer.
- **DO NOT** perform the reasoning steps yourself.
- Your hint must be a strategic suggestion (e.g., “focus on the audio first,” “compare the objects on the left and right,” “track the object’s movement over time”).

Example Hint: first locate the object making the sound, then count

Output: Provide ONLY the text of the hint.

Figure 13. The prompt template used to generate guiding hints for the main policy model.

Audio-Visual Localization Judge Prompt

You are a meticulous and precise Audio-Visual Grounding Evaluator. Your task is to provide a granular, stepwise evaluation of a model's attempt to localize an object based on audio and visual cues.

Given the following inputs, you will score the model's reasoning and final answer on several criteria.

[User Query]: {The user's original question to the model.}

[Audio Caption]: {A transcript of the relevant audio from the video clip.}

[Ground Truth Answer]: {The correct description and location of the target object.}

[Model's Reasoning]: {The reasoning process generated by the model inside its `<think>` tags.}

[Model's Final Answer]: {The final location and description from the model's `<answer>` tag.}

Your Task: Based on your analysis of all the provided information, you must evaluate the model's performance on the following four criteria. Provide your judgment as a single JSON object with a score from 0.0 (complete failure) to 1.0 (perfect) for each criterion.

- 1. Audio Cue Grounding (`audio_grounding_score`):** Did the model's reasoning correctly identify the key descriptive words in the [Audio Caption] that point to the target? (e.g., did it correctly identify "clapping" as the key sound?).
- 2. Visual Object Identification (`visual_id_score`):** Based on the audio cue, did the model's reasoning correctly identify the corresponding visual object in the scene? (e.g., after identifying "clapping," did it correctly identify the "audience" as the source?).
- 3. Location Accuracy (`location_acc_score`):** How accurate is the final spatial location (e.g., "Left," "Center") provided in the [Model's Final Answer] when compared to the [Ground Truth Answer]?
- 4. Caption Correctness (`caption_corr_score`):** How well does the model's final textual description of the object in its [Model's Final Answer] match the [Ground Truth Answer]?

Output Format: Return ONLY a single JSON object with your scores.

Example Output:

```
{'audio_grounding_score': 0.9, 'visual_id_score': 1.0,  
'location_acc_score': 1.0, 'caption_corr_score': 0.8}
```

Figure 14. The prompt template for our VLM-based judge in Stage 3. It guides the judge to produce a granular, stepwise reward by scoring the policy model's reasoning on audio grounding, visual identification, location accuracy, and caption correctness.



Query: Describe the relationship between the audio and visual elements in this video.

Baseline GRPO: The video shows a man and woman at a train station. **The man is wearing stripes** and the woman looks worried. **This suggests they might be in a relationship.** The train station setting indicates travel. The woman's expression shows concern which **could mean she's sad about departure.** The man sits on a bench so **he might be waiting for a train.** The dialogue mentions catching a train which confirms the travel theme. The woman eats an apple which shows she's passing time. **The close-up shot emphasizes emotion.** The voices have different tones indicating contrasting moods. **The striped shirt is distinctive** making the man easily identifiable. **Train stations are associated with goodbyes** so this is likely a farewell scene.

AVATAR: A **man in striped shirt and white gloves** walks towards a train while a **concerned woman** watches. He sits on a bench **appearing lost in thought**, she eats an apple with a **tense expression**. He approaches her from behind suggesting urgency. The scene ends with a **close-up of her face** with train in background symbolizing separation. Audio shows her tone shifting from calm to anxious while his voice remains gentle and soothing. Dialogue snippets ("Is that you?", "Sorry, I have a train to catch," "Very funny") indicate **identity check, abrupt departure, and sarcastic remark** respectively, creating a **tense, emotionally charged moment** at the train station.



Query: What emotions are conveyed through both the visual and audio elements?

Baseline GRPO: The video shows a man in a black beanie. **He looks worried** which **indicates stress.** There's also a woman with a bun. **She appears concerned** so **something bad might be happening.** The man is driving a car and **his posture suggests tension.** Gas stations are often used in movies for dramatic scenes. The audio has music that **sounds intense** which **creates suspense.** The man says "I'm sorry" which **means he feels bad.** Black clothing often symbolizes negativity. The woman's expression **shows she's upset** about **whatever situation they're in.** **Fast music usually indicates action or tension.** The overall combination suggests a thriller or drama genre.

AVATAR: From the video, I can see the man in the black beanie and jacket has a **tense expression**, **his eyes darting around**, and he looks anxious. The woman with the bun appears **concerned**. In the car, he's driving with **his head down and breathing heavily**, which suggests **guilt**. At the gas station, his interaction with the woman still feels tense. The overall atmosphere of the video is described as **tense and suspenseful**. From the audio, the man's **hurried and tense tone** when he speaks, especially when he repeatedly says "I'm sorry," further highlights his guilt. The **fast-paced, high-pitched music** in the background also contributes to the **tense mood**.

Figure 15. **Qualitative comparison between Baseline GRPO and AVATAR.** AVATAR demonstrates better **cross-modal integration** and **structured reasoning**, while Baseline GRPO shows **surface-level observations** and **disconnected audio-visual analysis**. Green highlighting shows AVATAR's effective synthesis of multimodal cues, red highlighting reveals GRPO's uniform credit assignment limitations.

```

1  def compute_avatar_loss(policy_logprobs: torch.Tensor,
2                           old_logprobs: torch.Tensor,
3                           advantages: torch.Tensor,
4                           completion_mask: torch.Tensor,
5                           lambda_tas: float,
6                           epsilon: float) -> torch.Tensor:
7
8      # 1. Standard GRPO Clipped Surrogate Objective
9      # -----
10     # Calculate the importance sampling ratio per token
11     ratio = torch.exp(policy_logprobs - old_logprobs)
12
13     # Clip the ratio to prevent excessively large policy updates
14     clipped_ratio = torch.clamp(ratio, 1 - epsilon, 1 + epsilon)
15
16     # The advantage is broadcasted to match the shape of the per-token ratios
17     advantages_per_token = advantages.unsqueeze(1)
18
19     # Calculate the unclipped and clipped surrogate losses per token
20     loss_unclipped = ratio * advantages_per_token
21     loss_clipped = clipped_ratio * advantages_per_token
22
23     # The standard per-token loss is the minimum of the two, negated
24     per_token_loss = -torch.min(loss_unclipped, loss_clipped)
25
26     # 2. Temporal Advantage Shaping (TAS)
27     # -----
28     # Create a tensor to hold the temporal weights, initialized to a baseline of 1.0
29     temporal_weights = torch.ones_like(per_token_loss)
30
31     # Calculate U-shaped weights for each sequence in the batch
32     for i in range(per_token_loss.size(0)):
33         seq_len = completion_mask[i].sum().item()
34         if seq_len > 1:
35             # Normalize token positions to a range of [0, 1]
36             positions = torch.arange(seq_len, device=per_token_loss.device, dtype=torch.
37             ← float32)
38             normalized_positions = positions / (seq_len - 1)
39
39             # U-Shaped Curve:  $y = 1.0 + \lambda \cdot (2x - 1)^2$ 
40             parabolic_curve = (2 * normalized_positions - 1)**2
41             u_curve_weights = 1.0 + (lambda_tas * parabolic_curve)
42
43             # Apply these weights to the relevant part of the sequence
44             temporal_weights[i, :seq_len] = u_curve_weights
45
46     # 3. Final Loss Calculation
47     # -----
48     # Apply the temporal weights to shape the credit assignment
49     shaped_per_token_loss = per_token_loss * temporal_weights
50
51     # Apply the completion mask to only consider the reasoning tokens
52     masked_loss = shaped_per_token_loss * completion_mask
53
54     # Aggregate the loss for the entire batch
55     final_loss = masked_loss.sum() / completion_mask.sum().clamp(min=1.0)
56
57     return final_loss

```

Listing 1. Pseudocode for TAS.